

Charged current deep-inelastic scattering at three loops

S. Moch and M. Rogal

*Deutsches Elektronensynchrotron DESY
Platanenallee 6, D-15738 Zeuthen, Germany*

Abstract

We derive for deep-inelastic neutrino(ν)-proton(P) scattering in the combination $\nu P - \bar{\nu} P$ the perturbative QCD corrections to three loops for the charged current structure functions F_2 , F_L and F_3 . In leading twist approximation we calculate the first five odd-integer Mellin moments in the case of F_2 and F_L and the first five even-integer moments in the case of F_3 . As a new result we obtain the coefficient functions to $O(\alpha_s^3)$ while the corresponding anomalous dimensions agree with known results in the literature.

1 Introduction

Predictions for structure functions in deep-inelastic scattering (DIS) including perturbative corrections in Quantum Chromodynamics (QCD) have recently been advanced to an unprecedented level of precision over a wide kinematical region of Bjorken x and $Q^2 = -q^2$, with q being the momentum of the exchanged gauge boson. The knowledge of the complete three-loop splitting functions for the scale evolution of unpolarized parton distributions of hadrons [1, 2] together with the second-order coefficient functions [3–7] has completed the next-to-next-to-leading order (NNLO) approximation of massless perturbative QCD for the DIS structure functions F_1 , F_2 and F_3 . In addition for electromagnetic (photon-exchange) DIS the three-loop coefficient functions for both F_2 and $F_L = F_2 - 2xF_1$ have become available [8, 9], the latter being actually required to complete the NNLO predictions, since the leading contribution to the coefficient functions is of first order in the strong coupling constant α_s .

In the present article, we extend the program of calculating higher order perturbative QCD corrections to the structure functions of charged current DIS. Our studies are motivated by the increasingly accurate measurements of neutral and charged current cross sections at HERA with a polarised beam of electrons and positrons [10–12]. At the same time we are also able to quantitatively improve predictions for physics at the front-end of a neutrino-factory, see e.g. Ref. [13]. To be specific, we consider neutrino-proton scattering in the combination $\nu P - \bar{\nu}P$, which corresponds to charged lepton-proton DIS as far as QCD corrections are concerned. Following Refs. [14–18] we compute the perturbative QCD predictions to three-loop accuracy for a number of fixed Mellin moments of the structure functions F_2 , F_L and F_3 .

Within the framework of the operator product expansion (OPE), and working in Mellin space, $F_2^{\nu P - \bar{\nu}P}$ and $F_L^{\nu P - \bar{\nu}P}$ are functions of odd Mellin moments only, while only even moments contribute to $F_3^{\nu P - \bar{\nu}P}$. This distinction between odd and even Mellin moments is opposite to the case of the neutral current structure functions and also to the case of charged current structure functions for neutrino-proton scattering in the combination $\nu P + \bar{\nu}P$. In the latter case, the three-loop results for $F_2^{\nu P + \bar{\nu}P}$ and $F_L^{\nu P + \bar{\nu}P}$ can be directly checked in electromagnetic DIS and taken over from Refs. [8, 9]. Also $F_3^{\nu P + \bar{\nu}P}$ is known to three-loop accuracy [19] with parametrizations for the respective coefficient functions given in Ref. [20].

Having available a limited number of fixed Mellin moments for F_2 , F_L and F_3 for both combinations of neutrino-proton scattering, i.e. $\nu P \pm \bar{\nu}P$ is a prerequisite for a subsequent complete calculation of the respective quantity to three loops. With the methods of Refs. [1, 2, 8, 9] at hand we have all ingredients for a future computation of the “all- n ” results in Mellin- n space, or equivalently the complete expression in Bjorken- x space after an inverse Mellin transform. However, applying the present results we can already comment on a number of phenomenological issues, which we do in a companion paper [21].

The outline of this article is as follows. In Section 2 we briefly recall our formalism, which is based on the optical theorem, the forward Compton amplitude and the OPE. Specifically we emphasize the symmetry properties of the Compton amplitude for neutral and charged current pro-

cesses and show how these select either odd or even Mellin moments for the structure functions F_2 , F_L and F_3 depending on the process under consideration, i.e. $\nu P \pm \bar{\nu} P$. In Section 3 we recall details of the renormalization and give all relevant details of the calculation in Section 4. Section 5 contains our results for the Mellin moments of $F_2^{\nu P - \bar{\nu} P}$, $F_L^{\nu P - \bar{\nu} P}$ and $F_3^{\nu P - \bar{\nu} P}$ in numerical form. Finally, we conclude in Section 6. The lengthy full expressions for the new moments of the coefficient functions are deferred to Appendix A and some details on the OPE are given in Appendix B.

2 General formalism

The subject of our calculation is unpolarized inclusive deep-inelastic lepton-nucleon scattering,

$$l(k) + \text{nucl}(p) \rightarrow l'(k') + X, \quad (2.1)$$

where $l(k), l'(k')$ are leptons of momenta k and k' , $\text{nucl}(p)$ denotes a nucleon of momenta p and X stands for all hadronic states allowed by quantum number conservation. In this article we are concentrating on charged current neutrino(ν)-proton(P) scattering, i.e. $\nu P, \bar{\nu} P$ via W^\pm boson exchange. As it is well known, the differential cross section for reaction (2.1) can be written as a product of leptonic $L_{\mu\nu}$ and hadronic $W_{\mu\nu}$ tensors

$$d\sigma \propto L^{\mu\nu} W_{\mu\nu}. \quad (2.2)$$

The leptonic tensor $L^{\mu\nu}$ for electroweak or pure electromagnetic gauge boson exchange is detailed in the literature, see e.g. Ref. [22] and will not be considered here. The hadronic tensor in Eq. (2.2) is given by

$$\begin{aligned} W_{\mu\nu}(p, q) &= \frac{1}{4\pi} \int d^4z e^{iq \cdot z} \langle \text{nucl}, p | J_\mu^\dagger(z) J_\nu(0) | \text{nucl}, p \rangle \\ &= e_{\mu\nu} \frac{1}{2x} F_L(x, Q^2) + d_{\mu\nu} \frac{1}{2x} F_2(x, Q^2) + i\epsilon_{\mu\nu\alpha\beta} \frac{p^\alpha q^\beta}{2p \cdot q} F_3(x, Q^2), \end{aligned} \quad (2.3)$$

where J_μ is either an electromagnetic or a weak current and $|\text{nucl}, p\rangle$ is the unpolarized hadronic state with momentum p . The boson transfers momentum q , $Q^2 = -q^2 > 0$, and the Bjorken scaling variable is defined as $x = Q^2/(2p \cdot q)$ with $0 < x \leq 1$. The tensors $e_{\mu\nu}$ and $d_{\mu\nu}$ are given by

$$e_{\mu\nu} = g_{\mu\nu} - \frac{q_\mu q_\nu}{q^2}, \quad (2.4)$$

$$d_{\mu\nu} = -g_{\mu\nu} - p_\mu p_\nu \frac{4x^2}{q^2} - (p_\mu q_\nu + p_\nu q_\mu) \frac{2x}{q^2}, \quad (2.5)$$

and $\epsilon_{\mu\nu\alpha\beta}$ is the totally antisymmetric tensor. The hadron structure functions F_i , $i = L, 1, 2, 3$ are the main subject of our investigations in the present paper, with F_1 being related to F_L and F_2 by the Callan-Gross relation,

$$F_L(x, Q^2) = F_2(x, Q^2) - 2xF_1(x, Q^2). \quad (2.6)$$

The structure function F_3 describes parity-violating effects that arise from vector and axial-vector interference and vanishes for pure electromagnetic interactions.

We are interested in the Mellin moments of the structure functions, defined as

$$F_i(n, Q^2) = \int_0^1 dx x^{n-2} F_i(x, Q^2), \quad i = 2, L; \quad (2.7)$$

$$F_3(n, Q^2) = \int_0^1 dx x^{n-1} F_3(x, Q^2). \quad (2.8)$$

The optical theorem relates the hadronic tensor in Eq. (2.3) to the imaginary part of the forward scattering amplitude of boson-nucleon scattering, $T_{\mu\nu}$,

$$W_{\mu\nu}(p, q) = \frac{1}{2\pi} \text{Im} T_{\mu\nu}(p, q). \quad (2.9)$$

The forward Compton amplitude $T_{\mu\nu}$ has a time-ordered product of two local currents, to which standard perturbation theory applies,

$$T_{\mu\nu}(p, q) = i \int d^4z e^{iq \cdot z} \langle \text{nucl}, p | T \left(J_\mu^\dagger(z) J_\nu(0) \right) | \text{nucl}, p \rangle. \quad (2.10)$$

In the Bjorken limit, $Q^2 \rightarrow \infty$, x fixed, the integral in Eq. (2.10) is dominated by the integration region near the light-cone $z^2 \sim 0$. In this region the phase in the exponent in Eq. (2.10) becomes stationary for the external momentum q being deep in the Euclidean region. Thus, we can use the OPE for a formal expansion of the current product in Eq. (2.10) around $z^2 \sim 0$ into a series of local composite operators of leading twist (see e.g. Ref. [23] for details). In terms of local operators for a time ordered product of the two electromagnetic or weak hadronic currents the OPE for Eq. (2.10) can be written in the following form

$$\begin{aligned} i \int d^4z e^{iq \cdot z} T \left(J_\mu^\dagger(z) J_\nu(0) \right) &= 2 \sum_{n,j} \left(\frac{2}{Q^2} \right)^n \left[\left(g_{\mu\nu} - \frac{q_\mu q_\nu}{q^2} \right) q_{\mu_1} q_{\mu_2} C_{L,j} \left(n, \frac{Q^2}{\mu^2}, \alpha_s \right) \right. \\ &\quad - \left(g_{\mu\mu_1} g_{\nu\mu_2} q^2 - g_{\mu\mu_1} q_\nu q_{\mu_2} - g_{\nu\mu_2} q_\mu q_{\mu_1} + g_{\mu\nu} q_{\mu_1} q_{\mu_2} \right) C_{2,j} \left(n, \frac{Q^2}{\mu^2}, \alpha_s \right) \\ &\quad \left. + i \varepsilon_{\mu\nu\mu_1\beta} g^{\beta\gamma} q_\gamma q_{\mu_2} C_{3,j} \left(n, \frac{Q^2}{\mu^2}, \alpha_s \right) \right] q_{\mu_3} \dots q_{\mu_n} O^{j, \{\mu_1, \dots, \mu_n\}}(\mu^2) + \text{higher twists}, \end{aligned} \quad (2.11)$$

where $j = \alpha, q, g$ and all quantities are assumed to be renormalized, μ being the renormalization scale. Higher twist contributions are omitted in Eq. (2.11) as they are less singular near the light-cone $z^2 \sim 0$ and suppressed by powers of $1/Q^2$. Therefore, the sum over n in Eq. (2.11) extends to infinity and runs only over the standard set of the spin- n twist-2 irreducible symmetrical and traceless operators. In a general case three kind of operators contribute (these correspond to the index j in Eq. (2.11)): the flavor non-singlet quark operators O^α , the flavor singlet quark operator

O^q and the flavor singlet gluon operator O^g . These are defined by,

$$O^{\alpha, \{\mu_1, \dots, \mu_n\}} = \bar{\Psi} \lambda^{\alpha} \gamma^{\{\mu_1} D^{\mu_2} \dots D^{\mu_n\}} \Psi, \quad \alpha = 1, 2, \dots, (n_f^2 - 1), \quad (2.12)$$

$$O^q_{\{\mu_1, \dots, \mu_n\}} = \bar{\Psi} \gamma^{\{\mu_1} D^{\mu_2} \dots D^{\mu_n\}} \Psi, \quad (2.13)$$

$$O^g_{\{\mu_1, \dots, \mu_n\}} = F^{\nu \{\mu_1} D^{\mu_2} \dots D^{\mu_{n-1}} F^{\mu_n\} \nu}. \quad (2.14)$$

Here, Ψ defines the quark operator and $F^{\mu\nu}$ the gluon operator. The generators of the flavor group $SU(n_f)$ are denoted by λ^α , and the covariant derivative by D^μ . It is understood that the symmetrical and traceless part is taken with respect to the indices in curly brackets.

The spin averaged operator matrix elements (OMEs) in Eqs. (2.12)–(2.14) sandwiched between some hadronic state are given by

$$\langle \text{nucl}, p | O^{j, \{\mu_1, \dots, \mu_n\}} | \text{nucl}, p \rangle = p^{\{\mu_1} \dots p^{\mu_n\}} A_{\text{nucl}}^j(n, \mu^2), \quad (2.15)$$

where hadron mass effects have been neglected. The OMEs themselves as given in Eq. (2.15) are not calculable in perturbative QCD, but they can be related to the quark and anti-quark distributions of a given flavor and to the gluon distribution in the hadron.

The scale evolution of the OMEs governed by anomalous dimensions is accessible to perturbative predictions as well as the coefficient functions $C_{i,j}$ multiplying the OMEs according to Eq. (2.11). Both the anomalous dimensions and the coefficient functions are calculable order by order in perturbative QCD in an expansion in the strong coupling constant α_s . In order to do so, we replace the nucleon state $|\text{nucl}, p\rangle$ in Eqs. (2.10), (2.11) by partonic states. In complete analogy to Eq. (2.10) we define the forward Compton amplitude $t_{\mu\nu}$ at parton level and the corresponding partonic OMEs,

$$\langle \text{parton}, p | O^{j, \{\mu_1, \dots, \mu_n\}} | \text{parton}, p \rangle = p^{\{\mu_1} \dots p^{\mu_n\}} A_{\text{parton}}^j(n, \mu^2). \quad (2.16)$$

As the OPE in Eq. (2.11) represents an operator relation, we derive the following parton level expression

$$\begin{aligned} t_{\mu\nu} &\equiv i \int d^4 z e^{iq \cdot z} \langle \text{parton}, p | T \left(J_\mu^\dagger(z) J_\nu(0) \right) | \text{parton}, p \rangle \\ &= 2 \sum_{n,j} \omega^n \left[e_{\mu\nu} C_{L,j} \left(n, \frac{Q^2}{\mu^2}, \alpha_s \right) + d_{\mu\nu} C_{2,j} \left(n, \frac{Q^2}{\mu^2}, \alpha_s \right) \right. \\ &\quad \left. + i \varepsilon_{\mu\nu\alpha\beta} \frac{p^\alpha q^\beta}{p \cdot q} C_{3,j} \left(n, \frac{Q^2}{\mu^2}, \alpha_s \right) \right] A_{\text{parton}}^j(n, \mu^2) + \text{higher twists}, \end{aligned} \quad (2.17)$$

which is an expansion in terms of the variable $\omega = (2p \cdot q)/Q^2 = 1/x$ for unphysical $\omega \rightarrow 0$ ($x \rightarrow \infty$). The coefficients $C_{i,j}$ with $i = 2, 3, L$ are of course the same as the previous ones appearing in Eqs. (2.11) and the scale evolution of the OMEs in Eq. (2.16) is controllable in perturbation theory.

Let us in the following recall a few aspects of flavor (isospin) symmetry of the DIS structure functions which are relevant to neutrino-nucleon scattering. The composite operators Eqs. (2.12)–(2.14) are either singlet or non-singlet operators referring to the representation of the $SU(n_f)$ flavor

group. In particular the non-singlet operator $O^{\alpha, \{\mu_1, \dots, \mu_n\}}$ in Eq. (2.12) contains the generators λ^α of the flavor $SU(n_f)$. It is well known, that for the separation of the singlet and non-singlet contributions to structure functions, Wilson coefficients, etc., one considers the sum and the difference of matrix elements for a proton P and a neutron N , e.g.

$$F_i^{eP \pm eN} \equiv F_i^{eP} \pm F_i^{eN}, \quad F_i^{\nu P \pm \nu N} \equiv F_i^{\nu P} \pm F_i^{\nu N}, \quad i = 2, 3, L. \quad (2.18)$$

The combination $P + N$ singles out contributions to the singlet (isoscalar) operators and $P - N$ the corresponding ones to the non-singlet (isovector) operators, which can be seen readily as follows. To that end, let us specialize for simplicity to the case of two flavors ($n_f = 2$) only, i.e. to a $SU(2)$ -isospin symmetry, the generalization to an arbitrary number n_f of flavors being straightforward. Then, in the $SU(2)$ example, the twist-two term Θ of the OPE consists of an isoscalar (θ_0) and isovector (θ_α) part, i.e.,

$$\Theta = \theta_0 \mathbf{1} + \theta_\alpha \lambda_\alpha, \quad \alpha = 1, 2, 3, \quad (2.19)$$

where $\mathbf{1}$ is unit matrix and $\lambda_\alpha = \sigma_\alpha/2$, σ_α are the usual Pauli matrices in fundamental representation. Sandwiching Eq. (2.19) between the proton $|P\rangle$ and neutron $|N\rangle$ states, one gets directly

$$\begin{aligned} \langle P|\Theta|P\rangle + \langle N|\Theta|N\rangle &= \theta_0 \langle P|P\rangle + \theta_\alpha \langle P|\lambda_\alpha|P\rangle + \theta_0 \langle N|N\rangle + \theta_\alpha \langle N|\lambda_\alpha|N\rangle \\ &= \theta_0 + \frac{1}{2}\theta_3 + \theta_0 - \frac{1}{2}\theta_3 = 2\theta_0, \end{aligned} \quad (2.20)$$

$$\langle P|\Theta|P\rangle - \langle N|\Theta|N\rangle = \theta_0 + \frac{1}{2}\theta_3 - (\theta_0 - \frac{1}{2}\theta_3) = \theta_3. \quad (2.21)$$

Here one uses the fact that proton and neutron are eigenvectors of the λ_3 isospin operator with eigenvalues $+1/2$ and $-1/2$, respectively. Hence the combinations of the OMEs such as $A_{P \pm N}^j(n) = A_P^j(n) \pm A_N^j(n)$ correspond to the isoscalar part (singlet contribution) and isovector part (non-singlet contribution), respectively. As an upshot one can conclude that the OPE for the $P - N$ combination receives contributions from non-singlet quark operator O^α Eq. (2.12), i.e. $j = \alpha$, in the r.h.s of Eq. (2.11). On the other hand, for the $P + N$ combination both singlet quark operator O^q Eq. (2.13) and singlet gluon operator O^g Eq. (2.14) contribute in the OPE, i.e. the sum on the r.h.s Eq. (2.11) runs over $j = q, g$.

Since in the present article, we are considering charged current DIS in the combination $\nu P - \bar{\nu}P$ we have due to isospin symmetry

$$\left. \begin{aligned} F_i^{\bar{\nu}P} &= F_i^{\nu N} \\ F_i^{\bar{\nu}N} &= F_i^{\nu P} \end{aligned} \right\} \Rightarrow F_i^{\nu P} - F_i^{\bar{\nu}P} = F_i^{\nu P} - F_i^{\nu N} = F_i^{\bar{\nu}N} - F_i^{\nu N}. \quad (2.22)$$

Thus, we are entirely restricted to non-singlet quark operators for the structure functions $F_2^{\nu P - \bar{\nu}P}$, $F_3^{\nu P - \bar{\nu}P}$ and $F_L^{\nu P - \bar{\nu}P}$.

Next, we would like to address the symmetry properties of the partonic forward Compton amplitude (2.17) $t_{\mu\nu}$ and explain how these translate into selection rules for either even or odd Mellin n -moments of the different DIS structure functions. To that end, let us inspect the Feynman diagrams for $t_{\mu\nu}$ at the leading order with initial quarks in Fig. 1. There the right diagram is simply

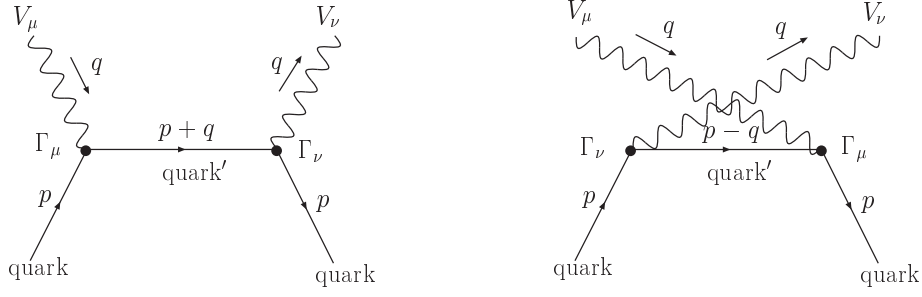


Figure 1: Leading order diagrams contributing to the forward Compton amplitude in deep-inelastic boson(V)-quark scattering.

the crossed diagram of the left one. In Fig. 1 we denote the gauge bosons by V_μ and V_ν . For the latter there are various choices as they can either be photons γ or weak gauge bosons Z^0 and W^\pm . The matrix element of the left diagram is proportional to

$$t_{\mu\nu} \propto \Gamma_\nu \not{D}(p+q) \Gamma_\mu, \quad (2.23)$$

where Γ_μ and Γ_ν denote the vertices of vector boson-fermion coupling, while $\not{D}(p+q)$ is the quark propagator of momentum $p+q$, $\not{D}(p+q) = -1/(\not{p} + \not{q})$. For the right diagram one has

$$t_{\mu\nu} \propto \Gamma_\mu \not{D}(p-q) \Gamma_\nu. \quad (2.24)$$

Under the simultaneous transformation $\mu \leftrightarrow \nu$ and $q \rightarrow -q$ the matrix element of the crossed diagram is equal to uncrossed one, provided both vertices Γ_μ and Γ_ν have the same structure.

Let us detail this situation for the case of the neutral current DIS first. The external bosons V_μ and V_ν in Fig. 1 being photons γ or Z^0 -bosons couple to the vertices Γ_μ and Γ_ν . The latter are either proportional to $e_q \gamma_\mu$ and $e_q \gamma_\nu$ with the fractional quark charge e_q (γ -boson) or to $(v_f \gamma_\mu + a_f \gamma_\mu \gamma_5)$ and $(v_f \gamma_\nu + a_f \gamma_\nu \gamma_5)$ with the (flavor-depended) vector and axial-vector current coupling constants v_f and a_f (Z^0 -boson). In the case of $\gamma - Z^0$ -interference one has to consider both, γ and Z^0 , in the initial state in Fig. 1 with a different gauge boson in the final state. In the end the effective number of diagrams for the interference contributions will be doubled. For all neutral current DIS cases the quark flavor, of course, remains conserved.

At this point, we can relate the action of simultaneously transforming $\mu \leftrightarrow \nu$ and $q \rightarrow -q$ in all Feynman diagrams contributing to $t_{\mu\nu}$ to the parameters of the OPE in Eq. (2.17), namely the coefficient functions C_2 , C_3 and C_L . It is clear that the full matrix element for $t_{\mu\nu}$ (l.h.s. of Eq. (2.17)) remains unchanged, since the transformation $\mu \leftrightarrow \nu$ and $q \rightarrow -q$ maps the crossed and uncrossed diagrams onto each other, even in the case of $\gamma - Z^0$ -interference due to the doubled number of diagrams. On the r.h.s of the OPE in Eq. (2.17) the tensors $e_{\mu\nu}$ and $d_{\mu\nu}$ remain invariant under $\mu \leftrightarrow \nu$, while the antisymmetric tensor $\epsilon_{\mu\nu\alpha\beta}$ picks up a sign (-1). The coefficients C_2 , C_3 and C_L as well as the OMEs A_{parton} , being Lorentz scalars, are at most functions of $Q^2 = -q^2$. Therefore they are invariant as well. Finally ω will be transformed to $-\omega$ (recall its definition $\omega = (2p \cdot q)/Q^2$). Thus, in the series expansion in spin n in Eq. (2.17) the coefficient functions C_2

and C_L are weighted by a factor $(-1)^n$, whereas C_3 is multiplied by $(-1)^{n+1}$. In other words, the sum in Eq. (2.17) runs for C_2 and C_L only over even Mellin moments n and only over odd for C_3 . The coefficients for other n have to vanish in Eq. (2.17). The same choice of n holds for the Mellin moments of the structure functions F_2 and F_L (even n) Eq. (2.7) and F_3 (odd n) Eq. (2.8) of neutral current DIS because of relations Eq. (2.30–2.31) which will be discussed later.

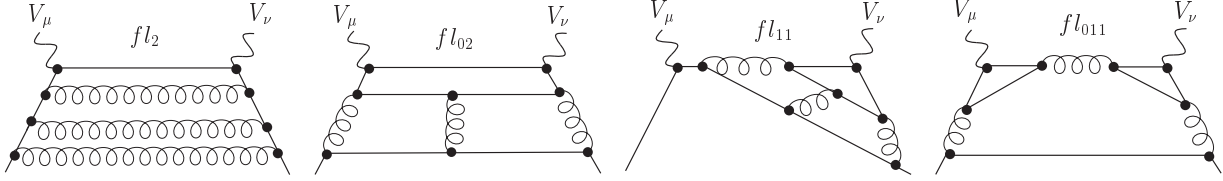


Figure 2: Representative three-loop diagrams for the various flavor classes in charged current neutrino-proton DIS (see text).

So far our discussion has been based on leading order Feynman diagrams but the previous arguments carry over to higher orders as well. Up to three-loop accuracy all Feynman diagrams fall in one of the so-called flavor classes fl_2 , fl_{02} , fl_{11} or fl_{011} displayed in Fig. 2. The class fl_2 corresponds to all diagrams with both gauge bosons V_μ and V_ν attached to the open fermion line of the initial (final) state quark. Class fl_{02} collects the diagrams with both gauge bosons attached to an internal closed fermion loop, while fl_{11} contains the diagrams with one boson attached to the closed loop and the other to the open line of the external quark. Finally the class fl_{011} denotes diagrams with both bosons attached to different closed quark loops. Depending on the process under consideration some flavor classes vanish identically. It is easy to see that the neutral current DIS assignments for C_2 and C_L (even Mellin moments) and C_3 (odd Mellin moments) from above persist and the same holds true for the structure functions.

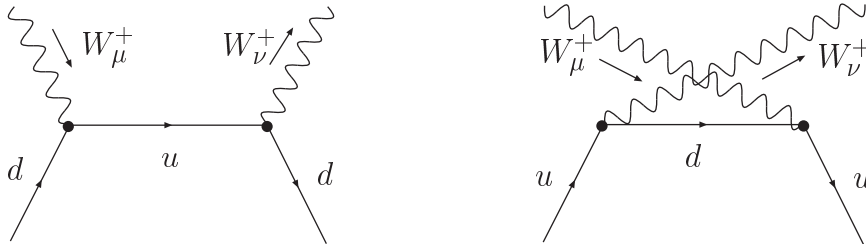


Figure 3: Leading order diagrams contributing to the forward Compton amplitude of charged current νP and νN scattering. The right diagram represents the crossed of the left one but with an incoming quark of different flavor.

Let us next turn to the case of charged current DIS. We have the structure functions F_2 , F_3 and F_L for both, an isoscalar and an isovector target, i.e. $\nu P \pm \nu N$, which we have to distinguish (see also Eq. (2.22)). On the partonic level this implies that we sum the contributions of u and d quarks in the singlet case and take their difference in the non-singlet case. For simplicity, we restrict

ourselves here again to $SU(2)$ -isospin symmetry with flavors u and d only. The generalization to s , c and more flavors should be clear. In charged current νP or νN DIS we are considering initial and final gauge bosons $V_\mu = W_\mu^+$ and $V_\nu = W_\nu^+$ (cf. Fig. 1), the coupling of d -quarks to W^- being excluded by electroweak theory. Say, we take d as incoming and outgoing quark in the left diagram of Fig. 1. Then, the scattering of W^+ with the incoming d quark yields a u quark (or c and t if more flavors are considered). On the other hand, the crossed diagram on the right in Fig. 1 simply does not exist for an incoming d quark, because it is not allowed by the electroweak Standard Model couplings. Rather, the incoming quark should be a u quark. In Fig. 3 we display explicitly the appropriate pair of Feynman diagrams at leading order.

Thus, for the partonic forward Compton amplitude (2.17) $t_{\mu\nu}$ in the combination $t_{\mu\nu}^{u+d} \equiv t_{\mu\nu}^u + t_{\mu\nu}^d$ we effectively sum the contributions of both, crossed and uncrossed, diagrams in Fig. 3 whereas for $t_{\mu\nu}^{u-d} \equiv t_{\mu\nu}^u - t_{\mu\nu}^d$ we subtract them. Then, we arrive at the following properties for simultaneous transformations $\mu \leftrightarrow \nu$ and $q \rightarrow -q$,

$$t_{\mu\nu}^{u+d} \rightarrow t_{\mu\nu}^{u+d}, \quad (2.25)$$

$$t_{\mu\nu}^{u-d} \rightarrow (-1)t_{\mu\nu}^{u-d}. \quad (2.26)$$

Eq. (2.25) implies that the forward Compton amplitude $t_{\mu\nu}^{u+d}$ has the same symmetry property as in the case of neutral current DIS. For the corresponding coefficient functions and their dependence on the Mellin variable n we may repeat exactly the same line of arguments as before leading to the conclusion that C_2 , C_L (C_3) are governed by even (odd) n only. In the other case, Eq. (2.26) shows that $t_{\mu\nu}^{u-d}$ is antisymmetric under the transformation $\mu \leftrightarrow \nu$ simultaneously with $q \rightarrow -q$, which gives an additional factor (-1) for the l.h.s. of Eq. (2.17). This alters the Mellin- n dependence of the coefficient functions so that we have precisely the opposite assignments, C_2 , C_L (C_3) being entirely odd (even) functions of n only.

Before moving on, let us briefly comment on the higher order diagrams for charged current DIS as illustrated in Fig. 2. For the flavor class fl_2 our tree level arguments from above may be literally repeated. In the flavor class fl_{02} , on the other hand, crossed diagrams with the same external quark flavor do contribute. However, this does not destroy the symmetry properties of the singlet and non-singlet combinations. The complete $t_{\mu\nu}^{u+d}$ simply sums the crossed and uncrossed diagrams and, therefore, is still symmetric under $\mu \leftrightarrow \nu$ simultaneously with $q \rightarrow -q$, thus Eq. (2.25) holds for the $u+d$ combination. In contrast, the contributions from the $u-d$ combination to the flavor class fl_{02} vanish. The flavor classes fl_{11} and fl_{011} are excluded in charged current DIS, because the flavor changes and, as a consequence, the coupling of one single W^+ -boson to a quark loop is not possible.

Finally, it remains to relate the coefficient functions C_2 , C_3 and C_L and the OMEs of Eq. (2.15) to the Mellin moments of structure functions. To that end, it is convenient to project Eq. (2.3) and the analogue of Eq. (2.17) for the hadron forward Compton amplitude $T_{\mu\nu}$ onto the respective Lorentz structure using projectors

$$P_L^{\mu\nu} \equiv -\frac{q^2}{(p \cdot q)^2} p^\mu p^\nu, \quad (2.27)$$

$$P_2^{\mu\nu} \equiv - \left(\frac{3-2\varepsilon}{2-2\varepsilon} \frac{q^2}{(p \cdot q)^2} p^\mu p^\nu + \frac{1}{2-2\varepsilon} g^{\mu\nu} \right), \quad (2.28)$$

$$P_3^{\mu\nu} \equiv -i \frac{1}{(1-2\varepsilon)(2-2\varepsilon)} \varepsilon^{\mu\nu\alpha\beta} \frac{p^\alpha q^\beta}{p \cdot q}, \quad (2.29)$$

where all expressions are exact in $D = 4 - 2\varepsilon$ dimensions.

With the help of Eqs. (2.27)–(2.29) one arrives at relations between Mellin moments of DIS structure functions (2.7), (2.8) and the parameters of OPE. On a technical level, this implies a Cauchy integration of the analogue of Eq. (2.17) for $T_{\mu\nu}$ in the complex ω -plane and we recall the necessary details in Appendix B.

$$\int_0^1 dx x^{n-2} F_i(x, Q^2) = \sum_j C_{i,j} \left(n, \frac{Q^2}{\mu^2}, \alpha_s \right) A_{\text{nucl}}^j(n, \mu^2), \quad i = 2, L, \quad (2.30)$$

$$\int_0^1 dx x^{n-1} F_3(x, Q^2) = \sum_j C_{3,j} \left(n, \frac{Q^2}{\mu^2}, \alpha_s \right) A_{\text{nucl}}^j(n, \mu^2). \quad (2.31)$$

To summarize, Eqs. (2.30) and (2.31) provide the basis to obtain Mellin moments of DIS structure functions in our approach relying on the OPE and the optical theorem. Furthermore, from the careful examination of the symmetry properties of the forward Compton amplitude $T_{\mu\nu}$ and, related, the underlying Feynman diagrams, we have deduced corresponding rules for the Mellin variable n . In the case of neutral current and charged current $\nu P + \nu N$ DIS the structure functions F_2 and F_L are only functions of even Mellin- n and only functions of odd n for F_3 . For the case of interest in this paper, charged current $\nu P - \nu N$ DIS, we encounter only odd functions in n for F_2 and F_L and, only even functions in n for F_3 , respectively.

3 Renormalization

In this Section we briefly recall the necessary steps in renormalizing the operators in the OPE and, following the discussion above, we restrict ourselves here entirely to the non-singlet case. Starting, say, from the partonic expression (2.17), i.e. partonic matrix elements of $t_{\mu\nu}$, we express the renormalized OMEs A_{parton}^j (see Eq. (2.16)) in terms of matrix elements of bare composite operators,

$$O^{\alpha, \text{ren}} = Z_{\text{ns}} O^{\alpha, \text{bare}}. \quad (3.1)$$

Here and later we suppress other indices and the explicit dependence on n for the operators (2.12). The scale dependence of the operator O^α is governed by the anomalous dimension γ_{ns} ,

$$\frac{d}{d \ln \mu^2} O^{\alpha, \text{ren}} \equiv -\gamma_{\text{ns}} O^{\alpha, \text{ren}}, \quad (3.2)$$

and is connected to the renormalization constant Z_{ns} in Eq. (3.1) by

$$\gamma_{\text{ns}} = - \left(\frac{d}{d \ln \mu^2} Z_{\text{ns}} \right) Z_{\text{ns}}^{-1}. \quad (3.3)$$

In order to arrive at explicit expressions for Z_{ns} or Eq. (3.3), one has to make use of a regularization procedure and a renormalization scheme. We choose dimensional regularization [24–27] in $D = 4 - 2\varepsilon$ dimensions and the modified minimal subtraction [28, 29] scheme, $\overline{\text{MS}}$. The running coupling evolves according to

$$\frac{d}{d \ln \mu^2} \frac{\alpha_s}{4\pi} \equiv \frac{d a_s}{d \ln \mu^2} = -\varepsilon a_s - \beta_0 a_s^2 - \beta_1 a_s^3 - \beta_2 a_s^4 - \dots, \quad (3.4)$$

and we have introduced the common short hand notation $a_s \equiv \alpha_s/(4\pi)$. The usual four-dimensional expansion coefficients β_n of the beta function in QCD read $\beta_0 = 11 - 2/3 n_f$ etc, with n_f representing the number of active quark flavors. The bare and the renormalized coupling, α_s^{bare} and α_s are related by

$$\alpha_s^{\text{bare}} = Z_{\alpha_s} \alpha_s, \quad (3.5)$$

where we have put the factor $S_\varepsilon = \exp(\varepsilon\{\ln(4\pi) - \gamma_E\}) = 1$ in the $\overline{\text{MS}}$ -scheme and the renormalization constant Z_{α_s} reads

$$Z_{\alpha_s} = 1 - \frac{\beta_0}{\varepsilon} a_s + \left(\frac{\beta_0^2}{\varepsilon^2} - \frac{\beta_1}{2\varepsilon} \right) a_s^2 + \dots. \quad (3.6)$$

In this framework, the renormalization factor Z_{ns} in Eq. (3.1) is a series of poles in $1/\varepsilon$, expressed in terms of β_n and the coefficients $\gamma^{(l)}$ of the anomalous dimensions from an expansion in a_s ,

$$\gamma(n) = \sum_{l=0}^{\infty} a_s^{l+1} \gamma^{(l)}(n). \quad (3.7)$$

Up to the third order in the coupling constant the expansion of Z_{ns} reads

$$\begin{aligned} Z_{\text{ns}} = & 1 + a_s \frac{1}{\varepsilon} \gamma_{\text{ns}}^{(0)} + a_s^2 \left[\frac{1}{2\varepsilon^2} \left\{ \left(\gamma_{\text{ns}}^{(0)} - \beta_0 \right) \gamma_{\text{ns}}^{(0)} \right\} + \frac{1}{2\varepsilon} \gamma_{\text{ns}}^{(1)} \right] \\ & + a_s^3 \left[\frac{1}{6\varepsilon^3} \left\{ \left(\gamma_{\text{ns}}^{(0)} - 2\beta_0 \right) \left(\gamma_{\text{ns}}^{(0)} - \beta_0 \right) \gamma_{\text{ns}}^{(0)} \right\} \right. \\ & \left. + \frac{1}{6\varepsilon^2} \left\{ 3\gamma_{\text{ns}}^{(0)} \gamma_{\text{ns}}^{(1)} - 2\beta_0 \gamma_{\text{ns}}^{(1)} - 2\beta_1 \gamma_{\text{ns}}^{(0)} \right\} + \frac{1}{3\varepsilon} \gamma_{\text{ns}}^{(2)} \right]. \quad (3.8) \end{aligned}$$

The anomalous dimensions $\gamma^{(l)}$ can thus be read off from the ε^{-1} terms of the renormalization factors at order a_s^{l+1} , while the higher poles in $1/\varepsilon$ can serve as checks for the calculation. The coefficient functions in Eqs. (2.11), (2.17), on the other hand, have an expansion in positive powers of ε ,

$$C_{i,\text{ns}} = \sum_{l=0}^{\infty} a_s^l \left(c_{i,\text{ns}}^{(l)} + \varepsilon a_{i,\text{ns}}^{(l)} + \varepsilon^2 b_{i,\text{ns}}^{(l)} + \dots \right), \quad (3.9)$$

where $i = 2, 3, L$ and we have again suppressed the dependence on n (and Q^2/μ^2). Here $C_{i,\text{ns}}$ is our generic notation for non-singlet contributions obtained for $C_{i,\alpha}$ in Eqs. (2.11), (2.17)

Due to the presence of γ_5 in the vertices, the axial-vector coupling in dimensional regularization brings up the need for additional renormalizations to restore the axial Ward-identities. This is extensively described in the literature and for the associated renormalizations we use the prescription of Ref. [30, 31] based on relating vector and axial-vector currents. The necessary constant Z_A for the axial renormalization Z_5 and the finite renormalization due to the treatment of γ_5 in the $\overline{\text{MS}}$ -scheme are known to three loops [30, 31].

The actual calculation of the anomalous dimension (3.2) and the coefficient functions $C_{i,\text{ns}}$ in perturbative QCD proceeds as follows. Using the Lorentz projectors (2.27)–(2.29) we obtain from the forward partonic Compton amplitude Eq. (2.17) the partonic invariants

$$t_{i,\text{ns}} = P_i^{\mu\nu} t_{\mu\nu}, \quad i = 2, 3, L, \quad (3.10)$$

see also Eqs. (B.1), (B.2). These invariants can be written in terms of the bare operator matrix elements as

$$t_{i,\text{ns}}(x, Q^2, \alpha_s, \varepsilon) = \quad (3.11)$$

$$2 \sum_n \left(\frac{1}{x}\right)^n C_{i,\text{ns}} \left(n, \frac{Q^2}{\mu^2}, \alpha_s, \varepsilon\right) Z_{\text{ns}} \left(\alpha_s, \frac{1}{\varepsilon}\right) A_{\text{q}}^{\text{ns,bare}} \left(n, \alpha_s, \frac{p^2}{\mu^2}, \varepsilon\right) + O(p^2),$$

where $i = 2, 3, L$ and the l.h.s. of Eq. (3.11) is renormalized by substituting the bare coupling constant in terms of the renormalized, see Eq. (3.5). The wave function renormalization for the external quark lines is an overall factor on both sides of the Eq. (3.11) and drops out. The terms $O(p^2)$ on the r.h.s. of Eq. (3.11) indicate higher twist contributions, which we neglect.

Starting with the partonic invariant $t_{i,\text{ns}}$ from Eq. (3.11), the renormalization constants Z_{ns} and the coefficient functions $C_{i,\text{ns}}$ are calculated using the method of projection developed in Ref. [32], which consists of applying the following projection operator,

$$\mathcal{P}_n[f(p, q)] \equiv \left[\frac{q^{\{\mu_1 \dots \mu_n\}}}{2n!} \frac{\partial^n}{\partial p^{\mu_1} \dots \partial p^{\mu_n}} f(p, q) \right] \Bigg|_{p=0}, \quad (3.12)$$

to both sides of Eq. (3.11). Here $q^{\{\mu_1 \dots \mu_n\}}$ is symmetrical and traceless, i.e. the harmonic part of the tensor $q^{\mu_1} \dots q^{\mu_n}$.

On the r.h.s. of Eq. (3.11), it is obvious, that the n -th order differentiation in the projection operator \mathcal{P}_n singles out precisely the n -th moment, i.e. the coefficient of $1/x^n$. All other powers of $1/x$ vanish either by differentiation or after nullifying the momentum p . The operator \mathcal{P}_n does not act on the renormalization constant Z_{ns} and the coefficient functions on the r.h.s. of Eq. (3.11) as they are only functions of n , α_s and ε . However, \mathcal{P}_n does act on the partonic bare OMEs $A_{\text{parton}}^{j,\text{bare}}$, where the nullification of p effectively eliminates all but the tree level diagrams $A_{\text{parton}}^{j,\text{tree}}$, because any diagram with loops becomes a massless tadpole and is put to zero in dimensional regularization. Finally, the $O(p^2)$ terms in Eq. (3.11), which denote higher twist contributions, become proportional to the metric tensor after differentiation. They are removed by the harmonic tensor $q^{\{\mu_1 \dots \mu_n\}}$. On the l.h.s. of Eq. (3.11), \mathcal{P}_n is applied to the integrands of all Feynman

diagrams contributing to the invariants $t_{i,\text{parton}}$. The momentum p is nullified before taking the limit $\varepsilon \rightarrow 0$, so that all infrared divergences as $p \rightarrow 0$ are dimensionally regularized for individual diagrams. This reduces the 4-point diagrams that contribute to $t_{\mu\nu}$ to self-energy type diagrams (2-point-functions) accessible to reduction algorithms such as MINCER [33] (see the Section 4).

To summarize, we find after application of the projection operator \mathcal{P}_n to Eq. (3.11)

$$\begin{aligned} t_{i,\text{ns}} \left(n, \frac{Q^2}{\mu^2}, \alpha_s, \varepsilon \right) &\equiv \mathcal{P}_n t_{i,\text{ns}}(x, Q^2, \alpha_s, \varepsilon) \\ &= C_{i,\text{ns}} \left(n, \frac{Q^2}{\mu^2}, \alpha_s, \varepsilon \right) Z_{\text{ns}} \left(\alpha_s, \frac{1}{\varepsilon} \right) A_{\text{q}}^{\text{ns},\text{tree}}(n, \varepsilon), \end{aligned} \quad (3.13)$$

where $i = 2, 3, L$. This is our starting point for an iterative determination of the anomalous dimensions and coefficient functions via the OPE, since the $C_{i,\text{ns}}$ (Z_{ns}) are expanded in positive (negative) powers of ε while the OME $A_{\text{q}}^{\text{ns},\text{tree}}$ does factorize after application of the projector \mathcal{P}_n . In a series expansion in terms of the renormalized coupling a_s at the scale $\mu^2 = Q^2$ we can write

$$t_{i,\text{ns}}(n) = \left(t_{i,\text{ns}}^{(0)}(n) + a_s t_{i,\text{ns}}^{(1)}(n) + a_s^2 t_{i,\text{ns}}^{(2)}(n) + a_s^3 t_{i,\text{ns}}^{(3)}(n) + \dots \right) A_{\text{q}}^{\text{ns},\text{tree}}(n), \quad (3.14)$$

with $i = 2, 3, L$ and recall that we use $a_s \equiv \alpha_s/(4\pi)$. Then we normalize leading order contribution as follows,

$$t_{i,\text{ns}}^{(0)}(n) = 1, \quad i = 2, 3, \quad \text{and} \quad t_{L,\text{ns}}^{(0)}(n) = 0, \quad (3.15)$$

where the OME $A_{\text{q}}^{\text{ns},\text{tree}}$ (being a constant) has been absorbed into the normalization of Eq. (3.15). With the normalization (3.15) one has

$$c_{i,\text{ns}}^{(0)}(n) = 1, \quad i = 2, 3, \quad \text{and} \quad c_{L,\text{ns}}^{(0)}(n) = 0. \quad (3.16)$$

At first order in α_s , expanding up to order ε^2 and suppressing the n -dependence from now on for brevity, we find

$$t_{i,\text{ns}}^{(1)} = \frac{1}{\varepsilon} \gamma_{\text{ns}}^{(0)} + c_{i,\text{ns}}^{(1)} + \varepsilon a_{i,\text{ns}}^{(1)} + \varepsilon^2 b_{i,\text{ns}}^{(1)} + O(\varepsilon^3), \quad i = 2, 3, \quad (3.17)$$

$$t_{L,\text{ns}}^{(1)} = c_{L,\text{ns}}^{(1)} + \varepsilon a_{L,\text{ns}}^{(1)} + \varepsilon^2 b_{L,\text{ns}}^{(1)} + O(\varepsilon^3). \quad (3.18)$$

Performing the expansion at α_s^2 up to order ε we arrive at the equations:

$$\begin{aligned} t_{i,\text{ns}}^{(2)} &= \frac{1}{2\varepsilon^2} \left\{ \left(\gamma_{\text{ns}}^{(0)} - \beta_0 \right) \gamma_{\text{ns}}^{(0)} \right\} + \frac{1}{2\varepsilon} \left\{ \gamma_{\text{ns}}^{(1)} + 2c_{i,\text{ns}}^{(1)} \gamma_{\text{ns}}^{(0)} \right\} \\ &+ c_{i,\text{ns}}^{(2)} + a_{i,\text{ns}}^{(1)} \gamma_{\text{ns}}^{(0)} + \varepsilon \left\{ a_{i,\text{ns}}^{(2)} + b_{i,\text{ns}}^{(1)} \gamma_{\text{ns}}^{(0)} \right\} + O(\varepsilon^2), \quad i = 2, 3, \end{aligned} \quad (3.19)$$

$$t_{L,\text{ns}}^{(2)} = \frac{1}{\varepsilon} \left\{ c_{L,\text{ns}}^{(1)} \gamma_{\text{ns}}^{(0)} \right\} + c_{L,\text{ns}}^{(2)} + a_{L,\text{ns}}^{(1)} \gamma_{\text{ns}}^{(0)} + \varepsilon \left\{ a_{L,\text{ns}}^{(2)} + b_{L,\text{ns}}^{(1)} \gamma_{\text{ns}}^{(0)} \right\} + O(\varepsilon^2).$$

Finally for the third order α_s^3 we obtain

$$\begin{aligned}
t_{i,\text{ns}}^{(3)} &= \frac{1}{6\epsilon^3} \left\{ \left(\gamma_{\text{ns}}^{(0)} - 2\beta_0 \right) \left(\gamma_{\text{ns}}^{(0)} - \beta_0 \right) \gamma_{\text{ns}}^{(0)} \right\} \\
&\quad \frac{1}{6\epsilon^2} \left\{ 3\gamma_{\text{ns}}^{(0)} \gamma_{\text{ns}}^{(1)} - 2\beta_0 \gamma_{\text{ns}}^{(1)} - 2\beta_1 \gamma_{\text{ns}}^{(0)} + 3c_{i,\text{ns}}^{(1)} \left(\gamma_{\text{ns}}^{(0)} - \beta_0 \right) \gamma_{\text{ns}}^{(0)} \right\} \\
&\quad + \frac{1}{6\epsilon} \left\{ 2\gamma_{\text{ns}}^{(2)} + 3c_{i,\text{ns}}^{(1)} \gamma_{\text{ns}}^{(1)} + 6c_{i,\text{ns}}^{(2)} \gamma_{\text{ns}}^{(0)} + 3a_{i,\text{ns}}^{(1)} \left(\gamma_{\text{ns}}^{(0)} - \beta_0 \right) \gamma_{\text{ns}}^{(0)} \right\} \\
&\quad + \frac{1}{2} \left\{ 2c_{i,\text{ns}}^{(3)} + a_{i,\text{ns}}^{(1)} \gamma_{\text{ns}}^{(1)} + 2a_{i,\text{ns}}^{(2)} \gamma_{\text{ns}}^{(0)} + b_{i,\text{ns}}^{(1)} \left(\gamma_{\text{ns}}^{(0)} - \beta_0 \right) \gamma_{\text{ns}}^{(0)} \right\} + O(\epsilon), \quad i = 2, 3,
\end{aligned} \tag{3.20}$$

$$\begin{aligned}
t_{L,\text{ns}}^{(3)} &= \frac{1}{2\epsilon^2} \left\{ c_{L,\text{ns}}^{(1)} \left(\gamma_{\text{ns}}^{(0)} - \beta_0 \right) \gamma_{\text{ns}}^{(0)} \right\} \\
&\quad + \frac{1}{2\epsilon} \left\{ c_{L,\text{ns}}^{(1)} \gamma_{\text{ns}}^{(1)} + 2c_{L,\text{ns}}^{(2)} \gamma_{\text{ns}}^{(0)} + a_{L,\text{ns}}^{(1)} \left(\gamma_{\text{ns}}^{(0)} - \beta_0 \right) \gamma_{\text{ns}}^{(0)} \right\} \\
&\quad + \frac{1}{2} \left\{ 2c_{L,\text{ns}}^{(3)} + a_{L,\text{ns}}^{(1)} \gamma_{\text{ns}}^{(1)} + 2a_{L,\text{ns}}^{(2)} \gamma_{\text{ns}}^{(0)} + b_{L,\text{ns}}^{(1)} \left(\gamma_{\text{ns}}^{(0)} - \beta_0 \right) \gamma_{\text{ns}}^{(0)} \right\} + O(\epsilon).
\end{aligned} \tag{3.21}$$

Eqs. (3.17)–(3.21) hold for both, even and odd Mellin moments alike and we did not distinguish these in our notation. However, from the discussion of the preceding Sections it is clear that the respective anomalous dimensions $\gamma^{(l)}$ and coefficient functions $c_{i,\text{ns}}^{(l)}$ describe different physical processes. In fact, it is well-known that starting from $\gamma^{(1)}$ and $c_{i,\text{ns}}^{(2)}$ (and $a_{i,\text{ns}}^{(2)}$, $b_{i,\text{ns}}^{(2)}$, etc.), they differ. The new results of the present paper from Eqs. (3.20), (3.21) at third order in α_s consist of odd Mellin moments for $c_{2,\text{ns}}^{(3)}$ and $c_{L,\text{ns}}^{(3)}$ and even moments for $c_{3,\text{ns}}^{(3)}$. Below in Sec. 4 we present numerical results for them, while complete expressions through rational numbers are deferred to Appendix A.

4 Calculation

In the previous Sections, we have laid the foundations to our calculation of Mellin moments of the DIS charged current structure functions $F_2^{\nu P-\bar{\nu}P}$, $F_3^{\nu P-\bar{\nu}P}$ and $F_L^{\nu P-\bar{\nu}P}$ together with their respective coefficient functions and anomalous dimensions. To that end, following Refs. [1, 2, 8, 9], we have calculated the Lorentz invariants of the parton Compton amplitude $t_{i,\text{ns}}^{(l)}$, $l = 0, 1, 2, 3$, $i = 2, 3, L$, as given in the l.h.s. of Eqs. (3.17)–(3.21) from first principles. All contributing Feynman diagram were generated and then projected by one of the Lorentz projection (2.27)–(2.29). Subsequently, the application of Eq. (3.12) for the harmonic projection \mathcal{P}_n extracts all contributions to the given Mellin moment, which are finally solved in terms of rational numbers, values of the Riemann zeta functions and $SU(N_c)$ color coefficients C_A , C_F and n_f . Due to the large number of diagrams involved in the calculations up to order α_s^3 sufficient automatization is necessary. Therefore the calculations are organized in detail as follows:

- All Feynman diagrams are generated automatically with the program QGRAF [34]. This program generates all possible Feynman diagrams (and topologies) for a given process in some

Lorentz invariant	Structure function	tree $O(\alpha_s^0)$	one-loop $O(\alpha_s^1)$	two-loop $O(\alpha_s^2)$	three-loop $O(\alpha_s^3)$	sum
$t_{2,\text{ns}}$	$F_2^{\nu P-\bar{\nu}P}$	1	4	55	1016	1076
$t_{L,\text{ns}}$	$F_L^{\nu P-\bar{\nu}P}$	1	4	55	1016	1076
$t_{3,\text{ns}}$	$F_3^{\nu P-\bar{\nu}P}$	1	4	63	1246	1314
in total						3466

Table 1: The number of diagrams involved in the calculation of the $\nu P - \bar{\nu}P$ charged current DIS structure functions F_2 , F_L and F_3 at tree level, one-loop, two-loop and three-loop, respectively.

special format. The program works very effectively, producing a database with thousands of diagrams within seconds only. For charged current DIS we have obtained from QGRAF 2, 10, 153 and 3468 diagrams for the tree, one-loop, two-loop and three-loop contributions, respectively.

- For all further calculations we have relied on the latest version of the symbolic manipulation program FORM [35, 36]. For the further treatment of QGRAF output, such as analysis of the topologies, the explicit implementation of Feynman rules etc. we have adapted a dedicated FORM procedure *conv.prc* from previous work, e.g. Ref. [9]. Most importantly, this procedure tries to exploit as many symmetry properties of the original Feynman diagrams in order to reduce their total number. The upshot of these efforts are presented in Table 1 order by order for structure function corresponding to the different Lorentz projections. As one can see, the number of diagrams obtained for $F_3^{\nu P-\bar{\nu}P}$ is always larger than for $F_2^{\nu P-\bar{\nu}P}$ or $F_L^{\nu P-\bar{\nu}P}$. The reason is that in the former case we can not apply certain symmetry transformations due to the presence of γ_5 in the vertices. The database for $F_2^{\nu P-\bar{\nu}P}$ and $F_L^{\nu P-\bar{\nu}P}$ produced by us does almost coincide with the one used in Ref. [16], except for small modifications. The database for $F_3^{\nu P-\bar{\nu}P}$ is completely new.
- For the calculation of the color factors for each Feynman diagram we have used the FORM package *color.h* [37].
- The actual calculation of the Mellin moments of the Feynman integrals has made use of MINCER. The detailed description of this program can be found in Ref. [33] for the FORM package *mincer.h*. For organization of the work of (a slightly modified version of) MINCER with the input databases we have used a dedicated database program MINOS [14, 15].
- Finally, on top of MINCER and MINOS some shell scripts managed the automatic runs of both programs for different parts of the calculation. This facilitates the bookkeeping of different input parameters for MINOS and MINCER due to different Lorentz projections,

orders of α_s etc in distributed running. Moreover, the shell scripts also organized the final summations over the flavor classes as well as the output of all final results.

Next, let us discuss the various checks we performed on the results of our calculations. First of all, we have tested our set-up by a recalculation of some known even Mellin moments for F_2 , F_L and odd moments for F_3 to find agreement with the published results of Refs. [9, 14–16]. Then, most importantly, we have checked gauge invariance, i.e. we calculated all our diagrams for all results for all Mellin moments presented in this article with a gauge parameter ξ for the gluon propagator,

$$i \frac{-g^{\mu\nu} + (1 - \xi)q^\mu q^\nu}{q^2}. \quad (4.1)$$

We kept all powers of ξ (up to ξ^4 in three loops for this calculation) through the entire calculation. Since parton structure functions are physical quantities any dependence on the gauge parameter ξ must disappear in the final result. This was indeed the case after summing all diagrams in a given flavor class. Furthermore, we have compared the anomalous dimensions γ_{ns} Eq. (3.2) as calculated by us from Eqs. (3.17)–(3.21) up to three loops with the results available in the literature [1] and found complete agreement for both, even and odd Mellin moments. In addition, the coefficient functions for the structure functions $F_i^{\nu P - \bar{\nu} P}$, $i = 2, 3, L$ at two loops are known from earlier work. Our two-loop results as obtained from Eq. (3.17)–(3.20) coincide with Refs. [3–7].

Finally, let us mention a few words on the hardware requirements. All calculations are CPU-time and disk space consuming, especially for the higher Mellin moments (higher n values). They were typically performed on an 64-bit AMD Opteron 2.2 GHz Linux machine with 4 GByte of memory. For example, the calculation of $t_{3,\text{ns}}$ for $n = 10$ took 56 days with the gauge parameter included, while the calculation of both, $t_{2,\text{ns}}$ and $t_{L,\text{ns}}$ for $n = 9$ on the same machine needed 33 days. For comparison, the calculation of lowest Mellin moment $n = 1$ for both projections $t_{2,\text{ns}}$ and $t_{L,\text{ns}}$ consumes less than a hour, whereas for $n = 2$ for $t_{3,\text{ns}}$ one needs approximately a couple of hours, always with the full gauge parameter dependence. At intermediate stages the calculations required also a large amount of disk space. Although the programs calculate diagrams one by one at the time the size of intermediate algebraic expressions for some diagrams can grow up to 20 GByte of a disk space (for instance for $n = 10$ three-loop diagrams). On the other hand, the final result for any of the Lorentz invariants occupies some KBytes only. With access to improved hardware, we plan to push the calculation further to $n = 16$, cf. Ref. [18].

5 Results

Following the steps outlined above in Sec. 4 we arrive at the results for the coefficient functions $C_{2,\text{ns}}$, $C_{L,\text{ns}}$ at the odd-integer values $n = 1, \dots, 9$, and for $C_{3,\text{ns}}$ at the even-integer values $n = 2, \dots, 10$, up to order α_s^3 . The third order expressions represent new results of this article. Using $a_s \equiv \alpha_s/(4\pi)$ and the shorthand notation for the n -th moment $C_{i,n}^{\text{ns}} \equiv C_{i,\text{ns}}(n)$ we find the following

numerical values at the scale $\mu_r = \mu_f = Q$,

$$C_{2,1}^{\text{ns}} = 1, \quad (5.1)$$

$$C_{2,3}^{\text{ns}} = 1 + 3.222222222 a_s + a_s^2 (72.32720288 - 11.125 n_f) + a_s^3 (1948.031519 - 496.5427343 n_f + 14.20173594 n_f^2), \quad (5.2)$$

$$C_{2,5}^{\text{ns}} = 1 + 8.725925925 a_s + a_s^2 (220.4151827 - 22.64048559 n_f) + a_s^3 (6925.814438 - 1347.125829 n_f + 32.94421923 n_f^2), \quad (5.3)$$

$$C_{2,7}^{\text{ns}} = 1 + 13.43677248 a_s + a_s^2 (386.2911104 - 33.10212484 n_f) + a_s^3 (13505.16600 - 2298.472900 n_f + 52.34745652 n_f^2), \quad (5.4)$$

$$C_{2,9}^{\text{ns}} = 1 + 17.47820105 a_s + a_s^2 (555.2720117 - 42.50367619 n_f) + a_s^3 (20990.73668 - 3278.689323 n_f + 71.31040423 n_f^2), \quad (5.5)$$

$$C_{L,1}^{\text{ns}} = +2.666666666 a_s + a_s^2 (61.33333333 - 4.740740740 n_f) + a_s^3 (2313.911655 - 405.2001359 n_f + 10.20576131 n_f^2), \quad (5.6)$$

$$C_{L,3}^{\text{ns}} = 1.333333333 a_s + a_s^2 (52.40384466 - 3.925925925 n_f) + a_s^3 (2584.178446 - 406.0509532 n_f + 11.59670781 n_f^2), \quad (5.7)$$

$$C_{L,5}^{\text{ns}} = +0.888888888 a_s + a_s^2 (44.23466187 - 3.012345679 n_f) + a_s^3 (2451.068575 - 360.6487058 n_f + 10.15089163 n_f^2), \quad (5.8)$$

$$C_{L,7}^{\text{ns}} = 0.666666666 a_s + a_s^2 (38.25090234 - 2.440740740 n_f) + a_s^3 (2290.679208 - 321.7773285 n_f + 8.868930041 n_f^2), \quad (5.9)$$

$$C_{L,9}^{\text{ns}} = 0.533333333 a_s + a_s^2 (33.82305394 - 2.056719576 n_f) + a_s^3 (2146.302724 - 290.9906309 n_f + 7.868039976 n_f^2), \quad (5.10)$$

$$C_{3,2}^{\text{ns}} = 1 - 1.777777777 a_s + a_s^2 (-47.07704646 - 0.09876543209 n_f) + a_s^3 (-2359.001407 + 305.2538856 n_f - 6.864103442 n_f^2), \quad (5.11)$$

$$C_{3,4}^{\text{ns}} = 1 + 4.866666666 a_s + a_s^2 (90.15322509 - 13.25902469 n_f) + a_s^3 (1478.747872 - 491.0449098 n_f + 11.77903924 n_f^2), \quad (5.12)$$

$$C_{3,6}^{\text{ns}} = 1 + 10.35132275 a_s + a_s^2 (258.8595696 - 25.14210054 n_f) + a_s^3 (7586.717646 - 1458.855783 n_f + 32.73965909 n_f^2), \quad (5.13)$$

$$C_{3,8}^{\text{ns}} = 1 + 14.90026455 a_s + a_s^2 (433.2106396 - 35.58166191 n_f) + a_s^3 (14862.60949 - 2469.591886 n_f + 53.25812942 n_f^2), \quad (5.14)$$

$$C_{3,10}^{\text{ns}} = 1 + 18.79152477 a_s + a_s^2 (605.9424494 - 44.87506803 n_f) + a_s^3 (22806.38215 - 3482.933316 n_f + 72.83344233 n_f^2). \quad (5.15)$$

Exact analytical expressions of these moments also with complete dependence on the color coefficients are given in Appendix A.

As was mentioned before, the two-loop coefficient functions in Eqs. (5.1)–(5.15) agree with

the results in Refs. [3–7]. In addition, Eq. (5.1) for $C_{2,1}^{\text{ns}}$ is nothing else but a manifestation of the Adler sum rule for DIS structure functions,

$$\int_0^1 \frac{dx}{x} \left(F_2^{\text{v}P}(x, Q^2) - F_2^{\text{v}N}(x, Q^2) \right) = 2, \quad (5.16)$$

which measures the isospin of the nucleon in the quark-parton model and does not receive any perturbative or non-perturbative corrections in QCD, see e.g. the discussion in Ref. [38]. Therefore, Eq. (5.1) is another important check of the correctness of our results.

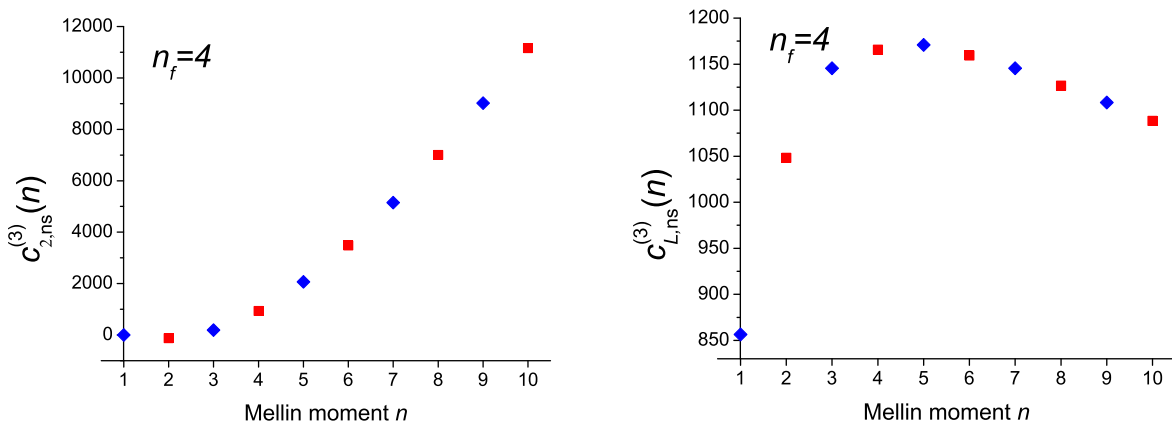


Figure 4: The first ten integer Mellin moments of the third order non-singlet coefficient functions $c_{2,\text{ns}}^{(3)}$ (left) and $c_{L,\text{ns}}^{(3)}$ (right) for charged current DIS with $n_f = 4$ flavors. For the even moments, the flavor class fl_{02} has been omitted, i.e. $fl_{02} = 0$ (see also the discussion in Sec. 2).

For illustration, let us plot the Mellin moments of the coefficient functions $c_{2,\text{ns}}^{(3)}$, $c_{3,\text{ns}}^{(3)}$ and $c_{L,\text{ns}}^{(3)}$ at three loops. The new non-singlet results (blue diamonds in Figs. 4 and 5) exhibit a similar smooth pattern as the known results (red squares in Figs. 4 and 5). Thus, it is feasible to use these moments for an approximate analytic reconstruction of the yet unknown coefficient functions $c_{i,\text{ns}}^{(3)}$ for $(\text{v}P - \bar{\text{v}}P)$ -DIS prior to “all- n ” calculation and similar to e.g. Refs. [36, 39]. We will do so in a companion paper [21].

Furthermore, we see that the respective values for odd and even moments, for instance on the left in Fig. 4 do confirm that differences between $c_{2,\text{ns}}^{(3)\text{v}P+\bar{\text{v}}P}$ and $c_{2,\text{ns}}^{(3)\text{v}P-\bar{\text{v}}P}$ are numerically small. This observation (see Fig. 5) provides also a posteriori justification for the extrapolation procedure from odd to even moments for C_3 in Refs. [40, 41]. There, available information on odd moments [16] used in fits of CCFR data [42] to the structure function xF_3 at NNLO in QCD and beyond. A further discussion of this and related issues is given in Ref. [21].

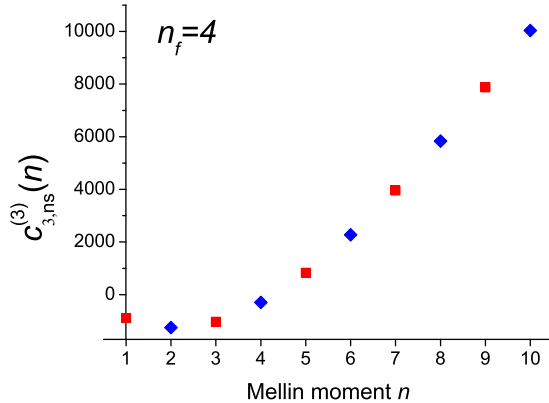


Figure 5: The first ten integer Mellin moments of the third order non-singlet coefficient functions $c_{3,\text{ns}}^{(3)}$ for charged current DIS with $n_f = 4$ flavors. For the odd moments, the flavor class fl_{02} has been omitted, i.e. $fl_{02} = 0$ (see also the discussion in Sec. 2).

6 Conclusions

In the present paper we have presented new results for Mellin moments of the charged current DIS structure functions $F_2^{\nu P - \bar{\nu} P}$, $F_L^{\nu P - \bar{\nu} P}$ and $F_3^{\nu P - \bar{\nu} P}$ including the perturbative QCD corrections to three loops. In the former case (F_2 , F_L) we have computed the first five odd-integer Mellin moments while in the latter case (F_3), the first five even-integer moments have been given. Our efforts are part of an ongoing program [1–9, 14–18] to calculate perturbative QCD corrections of all DIS structure functions to three-loop accuracy.

Within the framework of the OPE and the optical theorem we have calculated Feynman diagrams of the forward Compton amplitude $T_{\mu\nu}$ in Mellin space. In our presentation we have emphasized the symmetry properties of $T_{\mu\nu}$ and their relation to charged current $\nu P \pm \bar{\nu} P$ DIS, which was a crucial point in setting up the databases of Feynman diagrams. We have performed various checks on our computation. Most prominently, we have kept all powers of the gauge parameter ξ throughout the entire calculation to check that any ξ -dependence vanishes in our final results. Furthermore, we agree with the literature as far as the two-loop coefficient functions [3–7] and the three-loop anomalous dimensions [1] are concerned.

The discussion of phenomenological consequences of our Mellin space results is deferred to Ref. [21]. Future research will be devoted to the calculation of some higher Mellin moments, potentially $n = 11, \dots, 16$, depending on the available hardware infrastructure. Subsequently, we will also focus on an “all- n ” calculation in Mellin- n space with methods of Refs. [1, 2, 8, 9], since all databases for Feynman diagrams contributing to $F_2^{\nu P - \bar{\nu} P}$, $F_3^{\nu P - \bar{\nu} P}$ and $F_L^{\nu P - \bar{\nu} P}$ are available now.

FORM files of these results can be obtained from the preprint server <http://arXiv.org> by downloading the source of this article. Furthermore they are available from the authors upon

request.

Acknowledgments: We are grateful to J. Vermaseren and A. Vogt for useful discussions and to A. Vogt for valuable comments on the manuscript. The figures have been prepared with the packages AXODRAW [43] and JAXODRAW [44]. We acknowledge support by the Helmholtz Gemeinschaft under contract VH-NG-105 and in part by the Deutsche Forschungsgemeinschaft in Sonderforschungsbereich/Transregio 9.

A Appendix

In this Appendix we present the analytic expressions up to order a_s^3 for the coefficient functions $C_2^{\text{ns}}, C_L^{\text{ns}}$ at the odd-integer values $n = 1, \dots, 9$ and for C_3^{ns} at the even-integer values $n = 2, \dots, 10$. The notation follows Sec. 5 with C_A and C_F being the standard QCD colour factors, $C_A \equiv N_c = 3$ and $C_F = (N_c^2 - 1)/(2N_c) = 4/3$, and ζ_i stands for Riemann's ζ -function. The coefficient functions for the structure function F_2 at the scale $\mu_r = \mu_f = Q$ are given by

$$C_{2,1}^{\text{ns}} = 1, \tag{A.1}$$

$$C_{2,3}^{\text{ns}} = 1 \tag{A.2}$$

$$\begin{aligned} & + a_s C_F \frac{29}{12} \\ & + a_s^2 C_F n_f \left(-\frac{267}{32} \right) \\ & + a_s^2 C_F^2 \left(-\frac{217235}{10368} + 36\zeta_3 \right) \\ & + a_s^2 C_A C_F \left(\frac{25855}{432} - 43\zeta_3 \right) \\ & + a_s^3 C_F n_f^2 \left(\frac{641563}{69984} + \frac{100}{81}\zeta_3 \right) \\ & + a_s^3 C_F^2 n_f \left(-\frac{35314337}{699840} - \frac{1577}{45}\zeta_3 + \frac{50}{3}\zeta_4 \right) \\ & + a_s^3 C_F^3 \left(\frac{57093841}{373248} + \frac{103235}{324}\zeta_3 + \frac{55}{3}\zeta_4 - \frac{1520}{3}\zeta_5 \right) \\ & + a_s^3 C_A C_F n_f \left(-\frac{132494393}{699840} + \frac{39203}{405}\zeta_3 - \frac{50}{3}\zeta_4 \right) \\ & + a_s^3 C_A C_F^2 \left(-\frac{614328541}{2799360} + \frac{16171}{45}\zeta_3 - \frac{55}{2}\zeta_4 + 40\zeta_5 \right) \\ & + a_s^3 C_A^2 C_F \left(\frac{490358569}{699840} - \frac{344929}{405}\zeta_3 + \frac{55}{6}\zeta_4 + \frac{1070}{3}\zeta_5 \right), \\ C_{2,5}^{\text{ns}} = 1 \tag{A.3} \end{aligned}$$

$$\begin{aligned} & + a_s C_F \frac{589}{90} \\ & + a_s^2 C_F n_f \left(-\frac{2750819}{162000} \right) \end{aligned}$$

$$\begin{aligned}
& + a_s^2 C_F^2 \left(-\frac{30297101}{1620000} + 52\zeta_3 \right) \\
& + a_s^2 C_A C_F \left(\frac{35848409}{324000} - \frac{312}{5}\zeta_3 \right) \\
& + a_s^3 C_F n_f^2 \left(\frac{10958051}{486000} + \frac{728}{405}\zeta_3 \right) \\
& + a_s^3 C_F^2 n_f \left(-\frac{38720716199}{255150000} - \frac{257668}{4725}\zeta_3 + \frac{364}{15}\zeta_4 \right) \\
& + a_s^3 C_F^3 \left(\frac{132383443837}{2187000000} + \frac{5617861}{10125}\zeta_3 + \frac{1414}{75}\zeta_4 - 568\zeta_5 \right) \\
& + a_s^3 C_A C_F n_f \left(-\frac{50351664421}{122472000} + \frac{2187697}{14175}\zeta_3 - \frac{364}{15}\zeta_4 \right) \\
& + a_s^3 C_A C_F^2 \left(\frac{9620298263}{63787500} + \frac{10624153}{23625}\zeta_3 - \frac{707}{25}\zeta_4 - 108\zeta_5 \right) \\
& + a_s^3 C_A^2 C_F \left(\frac{230304417311}{163296000} - \frac{16031641}{11340}\zeta_3 + \frac{707}{75}\zeta_4 + 560\zeta_5 \right),
\end{aligned}$$

$$C_{2,7}^{\text{ns}} = 1 \tag{A.4}$$

$$\begin{aligned}
& + a_s C_F \frac{50791}{5040} \\
& + a_s^2 C_F n_f \left(-\frac{22072232029}{889056000} \right) \\
& + a_s^2 C_F^2 \left(-\frac{430403824451}{248935680000} + \frac{318}{5}\zeta_3 \right) \\
& + a_s^2 C_A C_F \left(\frac{549422934719}{3556224000} - \frac{5307}{70}\zeta_3 \right) \\
& + a_s^3 C_F n_f^2 \left(\frac{12315998504291}{336063168000} + \frac{2054}{945}\zeta_3 \right) \\
& + a_s^3 C_F^2 n_f \left(\frac{-1296360189717461}{4356374400000} - \frac{9299357}{132300}\zeta_3 + \frac{1027}{35}\zeta_4 \right) \\
& + a_s^3 C_F^3 \left(-\frac{1047772544741425169}{43912253952000000} + \frac{31380651109}{37044000}\zeta_3 + \frac{92741}{4900}\zeta_4 - \frac{4388}{7}\zeta_5 \right) \\
& + a_s^3 C_A C_F n_f \left(-\frac{4190308663484983}{6721263360000} + \frac{722354}{3675}\zeta_3 - \frac{1027}{35}\zeta_4 \right) \\
& + a_s^3 C_A C_F^2 \left(\frac{1465360668753075349}{18819537408000000} + \frac{33630683}{82320}\zeta_3 - \frac{278223}{9800}\zeta_4 - \frac{1376}{7}\zeta_5 \right) \\
& + a_s^3 C_A^2 C_F \left(\frac{873626018834459}{420078960000} - \frac{813517799}{441000}\zeta_3 + \frac{92741}{9800}\zeta_4 + \frac{4866}{7}\zeta_5 \right),
\end{aligned}$$

$$C_{2,9}^{\text{ns}} = 1 \tag{A.5}$$

$$\begin{aligned}
& + a_s C_F \frac{165169}{12600} \\
& + a_s^2 C_F n_f \left(-\frac{382605001967}{12002256000} \right) \\
& + a_s^2 C_F^2 \left(\frac{4711040116777}{201637900800} + \frac{510}{7}\zeta_3 \right)
\end{aligned}$$

$$\begin{aligned}
& + a_s^2 C_A C_F \left(\frac{946052961283}{4898880000} - \frac{1810}{21} \zeta_3 \right) \\
& + a_s^3 C_F n_f^2 \left(\frac{3438632355495191}{68052791520000} + \frac{4180}{1701} \zeta_3 \right) \\
& + a_s^3 C_F^2 n_f \left(-\frac{73610396284048043863}{157201948411200000} - \frac{281314024}{3274425} \zeta_3 + \frac{2090}{63} \zeta_4 \right) \\
& + a_s^3 C_F^3 \left(-\frac{202884354298201249627}{4001504141376000000} + \frac{110079158608}{93767625} \zeta_3 + \frac{1253219}{66150} \zeta_4 - 708 \zeta_5 \right) \\
& + a_s^3 C_A C_F n_f \left(-\frac{31467396414071567}{38192893200000} + \frac{1515609253}{6548850} \zeta_3 - \frac{2090}{63} \zeta_4 \right) \\
& + a_s^3 C_A C_F^2 \left(\frac{883676953019117176289}{571643448768000000} + \frac{6226321733}{20837250} \zeta_3 - \frac{1253219}{44100} \zeta_4 - \frac{2078}{9} \zeta_5 \right) \\
& + a_s^3 C_A^2 C_F \left(\frac{73714919752951175633}{27221116608000000} - \frac{872558077}{396900} \zeta_3 + \frac{1253219}{132300} \zeta_4 + \frac{49774}{63} \zeta_5 \right).
\end{aligned}$$

The coefficient functions for the structure function F_L at the scale $\mu_r = \mu_f = Q$ are given by

$$C_{L,1}^{\text{ns}} = a_s C_F^2 \tag{A.6}$$

$$\begin{aligned}
& + a_s^2 C_F n_f \left(-\frac{32}{9} \right) \\
& + a_s^2 C_F^2 \left(-11 \right) \\
& + a_s^2 C_A C_F \frac{182}{9} \\
& + a_s^3 C_F n_f^2 \frac{620}{81} \\
& + a_s^3 C_F^2 n_f \left(\frac{335}{9} - \frac{16}{3} \zeta_3 \right) \\
& + a_s^3 C_F^3 \left(313 + 752 \zeta_3 - 1120 \zeta_5 \right) \\
& + a_s^3 C_A C_F n_f \left(-\frac{8470}{81} + \frac{112}{3} \zeta_3 - \frac{160}{3} \zeta_5 \right) \\
& + a_s^3 C_A C_F^2 \left(-\frac{5462}{9} - \frac{2912}{3} \zeta_3 + 1520 \zeta_5 \right) \\
& + a_s^3 C_A^2 C_F \left(\frac{33140}{81} + 160 \zeta_3 - 320 \zeta_5 \right),
\end{aligned}$$

$$C_{L,3}^{\text{ns}} = a_s C_F \tag{A.7}$$

$$\begin{aligned}
& + a_s^2 C_F n_f \left(-\frac{53}{18} \right) \\
& + a_s^2 C_F^2 \left(-\frac{607}{24} + 24 \zeta_3 \right) \\
& + a_s^2 C_A C_F \left(\frac{467}{18} - 12 \zeta_3 \right) \\
& + a_s^3 C_F n_f^2 \frac{1409}{162} \\
& + a_s^3 C_F^2 n_f \left(\frac{403511}{4320} - \frac{1496}{15} \zeta_3 \right)
\end{aligned}$$

$$\begin{aligned}
& + a_s^3 C_F^3 \left(\frac{2898181}{10368} + \frac{2434}{9} \zeta_3 - 560 \zeta_5 \right) \\
& + a_s^3 C_A C_F n_f \left(-\frac{253051}{1620} + \frac{2488}{45} \zeta_3 \right) \\
& + a_s^3 C_A C_F^2 \left(-\frac{979877}{1080} + \frac{22184}{45} \zeta_3 + 360 \zeta_5 \right) \\
& + a_s^3 C_A^2 C_F \left(\frac{4262777}{6480} - \frac{1796}{5} \zeta_3 - 40 \zeta_5 \right), \\
C_{L,5}^{\text{ns}} &= a_s C_F \frac{2}{3} \tag{A.8}
\end{aligned}$$

$$\begin{aligned}
& + a_s^2 C_F n_f \left(-\frac{61}{27} \right) \\
& + a_s^2 C_F^2 \left(-\frac{119}{9} + 16 \zeta_3 \right) \\
& + a_s^2 C_A C_F \left(\frac{4861}{270} - 8 \zeta_3 \right) \\
& + a_s^3 C_F n_f^2 \frac{1850}{243} \\
& + a_s^3 C_F^2 n_f \left(\frac{5479121}{63000} - \frac{11128}{105} \zeta_3 \right) \\
& + a_s^3 C_F^3 \left(\frac{107779259}{2430000} + \frac{320}{3} \zeta_5 - \frac{64426}{675} \zeta_3 \right) \\
& + a_s^3 C_A C_F n_f \left(-\frac{48931997}{340200} + \frac{56318}{945} \zeta_3 \right) \\
& + a_s^3 C_A C_F^2 \left(-\frac{73036627}{113400} + \frac{3980216}{4725} \zeta_3 - 240 \zeta_5 \right) \\
& + a_s^3 C_A^2 C_F \left(\frac{784906033}{1360800} - \frac{278009}{630} \zeta_3 + \frac{280}{3} \zeta_5 \right), \\
C_{L,7}^{\text{ns}} &= a_s C_F \frac{1}{2} \tag{A.9}
\end{aligned}$$

$$\begin{aligned}
& + a_s^2 C_F n_f \left(-\frac{659}{360} \right) \\
& + a_s^2 C_F^2 \left(-\frac{2351887}{302400} + 12 \zeta_3 \right) \\
& + a_s^2 C_A C_F \left(\frac{2089693}{151200} - 6 \zeta_3 \right) \\
& + a_s^3 C_F n_f^2 \frac{43103}{6480} \\
& + a_s^3 C_F^2 n_f \left(\frac{1089629735311}{16003008000} - \frac{148192}{1575} \zeta_3 \right) \\
& + a_s^3 C_F^3 \left(-\frac{10999391897239}{99574272000} + 600 \zeta_5 - \frac{83782639}{220500} \zeta_3 \right) \\
& + a_s^3 C_A C_F n_f \left(-\frac{7151831837}{57153600} + \frac{10172}{189} \zeta_3 \right) \\
& + a_s^3 C_A C_F^2 \left(-\frac{17816756739419}{45722880000} + \frac{460935289}{441000} \zeta_3 - 700 \zeta_5 \right)
\end{aligned}$$

$$\begin{aligned}
& + a_s^3 C_A^2 C_F \left(\frac{1082520395023}{2286144000} - \frac{14765939}{31500} \zeta_3 + 200 \zeta_5 \right), \\
C_{L,9}^{\text{ns}} = & a_s C_F \frac{2}{5} \\
& + a_s^2 C_F n_f \left(-\frac{4859}{3150} \right) \\
& + a_s^2 C_F^2 \left(-\frac{3177697}{661500} + \frac{48}{5} \zeta_3 \right) \\
& + a_s^2 C_A C_F \left(\frac{7429883}{661500} - \frac{24}{5} \zeta_3 \right) \\
& + a_s^3 C_F n_f^2 \frac{836471}{141750} \\
& + a_s^3 C_F^2 n_f \left(\frac{17671408832087}{330062040000} - \frac{1439512}{17325} \zeta_3 \right) \\
& + a_s^3 C_F^3 \left(-\frac{5753430631305541}{25204737600000} - \frac{35201422}{55125} \zeta_3 + 1024 \zeta_5 \right) \\
& + a_s^3 C_A C_F n_f \left(-\frac{1186239473563}{10777536000} + \frac{17528393}{363825} \zeta_3 \right) \\
& + a_s^3 C_A C_F^2 \left(-\frac{174689016402059}{933508800000} + \frac{45254429}{36750} \zeta_3 - 1104 \zeta_5 \right) \\
& + a_s^3 C_A^2 C_F \left(\frac{88521637399093}{228614400000} - \frac{41525}{84} \zeta_3 + 296 \zeta_5 \right).
\end{aligned} \tag{A.10}$$

The coefficient functions for the structure function F_3 at the scale $\mu_r = \mu_f = Q$ are given by

$$\begin{aligned}
C_{3,2}^{\text{ns}} = & 1 \\
& + a_s C_F \left(-\frac{4}{3} \right) \\
& + a_s^2 C_F n_f \left(-\frac{2}{27} \right) \\
& + a_s^2 C_F^2 \frac{1016}{81} \\
& + a_s^2 C_A C_F \left(\frac{17}{9} - 16 \zeta_3 \right) \\
& + a_s^3 C_F n_f^2 \left(-\frac{13336}{2187} + \frac{64}{81} \zeta_3 \right) \\
& + a_s^3 C_F^2 n_f \left(-\frac{182014}{2187} + \frac{448}{9} \zeta_3 + \frac{32}{3} \zeta_4 \right) \\
& + a_s^3 C_F^3 \left(-\frac{55954}{729} - \frac{11584}{81} \zeta_3 + \frac{64}{3} \zeta_4 + \frac{640}{3} \zeta_5 \right) \\
& + a_s^3 C_A C_F n_f \left(\frac{156404}{2187} + \frac{1456}{81} \zeta_3 - \frac{32}{3} \zeta_4 \right) \\
& + a_s^3 C_A C_F^2 \left(\frac{855382}{2187} + \frac{56}{9} \zeta_3 - 32 \zeta_4 - 320 \zeta_5 \right) \\
& + a_s^3 C_A^2 C_F \left(-\frac{481450}{2187} - \frac{18728}{81} \zeta_3 + \frac{32}{3} \zeta_4 + \frac{800}{3} \zeta_5 \right),
\end{aligned} \tag{A.11}$$

$$C_{3,4}^{\text{ns}} = 1 \tag{A.12}$$

$$\begin{aligned}
& + a_s C_F \frac{73}{20} \\
& + a_s^2 C_F n_f \left(-\frac{1073981}{108000} \right) \\
& + a_s^2 C_F^2 \left(-\frac{59219099}{6480000} + 28\zeta_3 \right) \\
& + a_s^2 C_A C_F \left(\frac{3575579}{54000} - \frac{227}{5}\zeta_3 \right) \\
& + a_s^3 C_F n_f^2 \left(\frac{12195323}{1749600} + \frac{628}{405}\zeta_3 \right) \\
& + a_s^3 C_F^2 n_f \left(-\frac{18625311191}{109350000} + \frac{38021}{675}\zeta_3 + \frac{314}{15}\zeta_4 \right) \\
& + a_s^3 C_F^3 \left(-\frac{48030418393}{5832000000} + \frac{9183239}{40500}\zeta_3 + \frac{1439}{75}\zeta_4 - \frac{704}{3}\zeta_5 \right) \\
& + a_s^3 C_A C_F n_f \left(-\frac{529878917}{3499200} + \frac{29266}{405}\zeta_3 - \frac{314}{15}\zeta_4 \right) \\
& + a_s^3 C_A C_F^2 \left(\frac{1003904196083}{17496000000} - \frac{185929}{2250}\zeta_3 - \frac{1439}{50}\zeta_4 - 208\zeta_5 \right) \\
& + a_s^3 C_A^2 C_F \left(\frac{8293616147}{17496000} - \frac{1625431}{2025}\zeta_3 + \frac{1439}{150}\zeta_4 + \frac{1430}{3}\zeta_5 \right),
\end{aligned}$$

$$C_{3,6}^{\text{ns}} = 1 \tag{A.13}$$

$$\begin{aligned}
& + a_s C_F \frac{4891}{630} \\
& + a_s^2 C_F n_f \left(-\frac{1047784469}{55566000} \right) \\
& + a_s^2 C_F^2 \left(-\frac{15792028349}{3889620000} + \frac{228}{5}\zeta_3 \right) \\
& + a_s^2 C_A C_F \left(\frac{105144247}{889056} - \frac{2216}{35}\zeta_3 \right) \\
& + a_s^3 C_F n_f^2 \left(\frac{25846271107}{1166886000} + \frac{5672}{2835}\zeta_3 \right) \\
& + a_s^3 C_F^2 n_f \left(-\frac{57923821071217}{204205050000} + \frac{212692}{6615}\zeta_3 + \frac{2836}{105}\zeta_4 \right) \\
& + a_s^3 C_F^3 \left(-\frac{10620928547301491}{257298363000000} + \frac{2025255523}{3472875}\zeta_3 + \frac{69862}{3675}\zeta_4 - \frac{9944}{21}\zeta_5 \right) \\
& + a_s^3 C_A C_F n_f \left(-\frac{81497704436303}{210039480000} + \frac{1750321}{14175}\zeta_3 - \frac{2836}{105}\zeta_4 \right) \\
& + a_s^3 C_A C_F^2 \left(\frac{8198632169233}{8508543750} - \frac{4570231}{42875}\zeta_3 - \frac{34931}{1225}\zeta_4 - \frac{1236}{7}\zeta_5 \right) \\
& + a_s^3 C_A^2 C_F \left(\frac{345351668819093}{280052640000} - \frac{14709577}{11340}\zeta_3 + \frac{34931}{3675}\zeta_4 + \frac{12848}{21}\zeta_5 \right),
\end{aligned}$$

$$C_{3,8}^{\text{ns}} = 1 \tag{A.14}$$

$$+ a_s C_F \frac{56323}{5040}$$

$$\begin{aligned}
& + a_s^2 C_F n_f \left(-\frac{640590322783}{24004512000} \right) \\
& + a_s^2 C_F^2 \left(\frac{292667334922909}{20163790080000} + \frac{2046}{35} \zeta_3 \right) \\
& + a_s^2 C_A C_F \left(\frac{124690328633}{768144384} - \frac{16021}{210} \zeta_3 \right) \\
& + a_s^3 C_F n_f^2 \left(\frac{1011263478114371}{27221116608000} + \frac{19766}{8505} \zeta_3 \right) \\
& + a_s^3 C_F^2 n_f \left(-\frac{6152314125227207753}{14291086219200000} + \frac{1470167}{238140} \zeta_3 + \frac{9883}{315} \zeta_4 \right) \\
& + a_s^3 C_F^3 \left(-\frac{2725949924349586498181}{32012033131008000000} + \frac{2676254422397}{3000564000} \zeta_3 + \frac{2510407}{132300} \zeta_4 - 564 \zeta_5 \right) \\
& + a_s^3 C_A C_F n_f \left(-\frac{332470249596994151}{544422332160000} + \frac{198295567}{1190700} \zeta_3 - \frac{9883}{315} \zeta_4 \right) \\
& + a_s^3 C_A C_F^2 \left(\frac{724070773013223516571}{457314759014400000} - \frac{19725946973}{166698000} \zeta_3 - \frac{2510407}{88200} \zeta_4 - \frac{2132}{9} \zeta_5 \right) \\
& + a_s^3 C_A^2 C_F \left(\frac{528130813453946861}{272211166080000} - \frac{39055999}{22680} \zeta_3 + \frac{2510407}{264600} \zeta_4 + \frac{45994}{63} \zeta_5 \right),
\end{aligned}$$

$$C_{3,10}^{\text{ns}} = 1 \quad (\text{A.15})$$

$$\begin{aligned}
& + a_s C_F \frac{1953379}{138600} \\
& + a_s^2 C_F n_f \left(-\frac{537659500957277}{15975002736000} \right) \\
& + a_s^2 C_F^2 \left(\frac{597399446375524589}{14760902528064000} + \frac{7202}{105} \zeta_3 \right) \\
& + a_s^2 C_A C_F \left(\frac{5832602058122267}{29045459520000} - \frac{99886}{1155} \zeta_3 \right) \\
& + a_s^3 C_F n_f^2 \left(\frac{51339756673194617191}{996360920644320000} + \frac{48220}{18711} \zeta_3 \right) \\
& + a_s^3 C_F^2 n_f \left(-\frac{125483817946055121351353}{209235793335307200000} - \frac{59829376}{3274425} \zeta_3 + \frac{24110}{693} \zeta_4 \right) \\
& + a_s^3 C_F^3 \left(-\frac{744474223606695878525401307}{7088908678200207936000000} + \frac{28630985464358}{24960941775} \zeta_3 \right. \\
& \quad \left. + \frac{151796299}{8004150} \zeta_4 - \frac{53708}{99} \zeta_5 \right) \\
& + a_s^3 C_A C_F n_f \left(-\frac{185221350045507487753}{226445663782800000} + \frac{8071097}{39690} \zeta_3 - \frac{24110}{693} \zeta_4 \right) \\
& + a_s^3 C_A C_F^2 \left(\frac{19770078729338607732075449}{8369431733412288000000} - \frac{619383700181}{5546875950} \zeta_3 \right. \\
& \quad \left. - \frac{151796299}{5336100} \zeta_4 - \frac{37322}{99} \zeta_5 \right) \\
& + a_s^3 C_A^2 C_F \left(\frac{93798719639056648125143}{36231306205248000000} - \frac{43202630363}{20582100} \zeta_3 \right. \\
& \quad \left. + \frac{151796299}{16008300} \zeta_4 + \frac{195422}{231} \zeta_5 \right).
\end{aligned}$$

B Appendix

In this Appendix, we recall a few technical steps necessary to arrive at the relations (2.30), (2.31) between the parameters of OPE and the Mellin moments of DIS structure functions. To that end, we would like to put particular emphasis on the symmetry properties of the hadron forward Compton amplitude $T_{\mu\nu}(p, q)$ in Eq. (2.10) under the transformations $\mu \leftrightarrow \nu$ and $q \rightarrow -q$. Since our discussion in Sec. 2 was largely based on Feynman diagram considerations at parton level it remains to link the line of arguments to the OPE of Eq. (2.11), to the analogue of the OPE (2.17) for $T_{\mu\nu}$ and, eventually to the Mellin moments of F_2 , F_3 and F_L in Eqs. (2.7), (2.8).

Let us start by observing, that the OPE (2.11) for $T_{\mu\nu}$ gives rise to a series expansion in terms of ω similar to Eq. (2.17). This series being valid for unphysical $\omega = 1/x \rightarrow 0$ only (recall the Bjorken variable $0 < x \leq 1$) is related to the physical Mellin moments of F_2 , F_3 and F_L by means of a Cauchy integration. Here, the behavior of $T_{\mu\nu}$ under the mapping $\omega \rightarrow -\omega$ ($q \rightarrow -q$) becomes relevant. Applying the Lorentz projectors (2.27)–(2.29) to $T_{\mu\nu}$ we obtain

$$T_i(\omega, Q^2) \equiv P_L^{\mu\nu} T_{\mu\nu}(\omega, Q^2) = 2 \sum_{n,j} \omega^n C_{L,j} \left(n, \frac{Q^2}{\mu^2}, \alpha_s \right) A_{\text{nucl}}^j(n, \mu^2), \quad i = 2, L. \quad (\text{B.1})$$

In Sec. 2 we discussed which coefficients $C_{L,j}(n)$ survive in the OPE (2.11). As consequence the sum (B.1) runs over even n for the neutral current structure functions F_2 , F_L and the charged current (singlet) structure functions $F_2^{\nu P+\nu N}$, $F_L^{\nu P+\nu N}$ and therefore $T_i(-\omega, Q^2) = T_i(\omega, Q^2)$. For the charged current (non-singlet) structure functions $F_2^{\nu P-\nu N}$ and $F_L^{\nu P-\nu N}$ we sum over all odd n . Therefore $T_i(-\omega, Q^2) = -T_i(\omega, Q^2)$. Furthermore, we have

$$T_3(\omega, Q^2) \equiv P_3^{\mu\nu} T_{\mu\nu}(\omega, Q^2) = 2 \sum_{n,j} \omega^n C_{3,j} \left(n, \frac{Q^2}{\mu^2}, \alpha_s \right) A_{\text{nucl}}^j(n, \mu^2), \quad (\text{B.2})$$

where we sum over all odd n for the neutral current F_3 and charged current $F_3^{\nu P+\nu N}$. As consequence we have obviously $T_3(-\omega, Q^2) = -T_3(\omega, Q^2)$. On the other hand, for the charged current $F_3^{\nu P-\nu N}$ the sum runs over even n and therefore $T_3(-\omega, Q^2) = T_3(\omega, Q^2)$.

In applying the Cauchy integration to both sides of Eqs. (B.1), (B.2) with a contour C as shown in the Fig. 6 we exploit the fact that the Lorentz projected forward Compton amplitude is an analytic function of complex variable ω . The branch cuts extend along the real axis for $\omega \leq -1$ and $\omega \geq 1$ because of kinematical constraints from Bjorken x and symmetry properties. We divide both sides of Eqs. (B.1), (B.2) by $2\pi i \omega^m$ and pick up the appropriate residues on the r.h.s according to

$$\frac{1}{2\pi i} \oint_C d\omega \frac{\omega^n}{\omega^m} = \delta_{n,m-1}. \quad (\text{B.3})$$

For the l.h.s. one obtains

$$\frac{1}{2\pi i} \oint_C \frac{d\omega}{\omega^m} T_i(\omega, Q^2) = \frac{1}{2\pi i} \left(+ \int_{+\infty-i\epsilon}^{+1-i\epsilon} + \int_{+1+i\epsilon}^{+\infty+i\epsilon} + \int_{-\infty+i\epsilon}^{-1+i\epsilon} + \int_{-1-i\epsilon}^{-\infty-i\epsilon} \right) \frac{d\omega}{\omega^m} T_i(\omega, Q^2) \quad (\text{B.4})$$

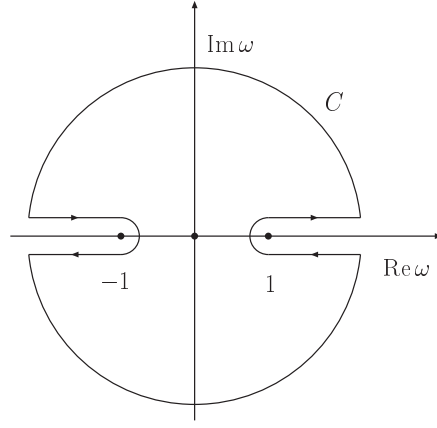


Figure 6: The contour C of the Cauchy integration in the complex ω -plane.

$$\begin{aligned}
&= \frac{1}{\pi i} \left(- \int_{+1-i\epsilon}^{+\infty-i\epsilon} + \int_{+1+i\epsilon}^{+\infty+i\epsilon} \right) \frac{d\omega}{\omega^m} T_i(\omega, Q^2) \\
&= \frac{2}{\pi} \int_1^{+\infty} \frac{d\omega}{\omega^m} \text{Im} T_i(\omega, Q^2), \quad i = 2, 3, L,
\end{aligned}$$

where we have used that for the physical cases with either even or odd n in Eqs. (B.1), (B.2) the whole combination $(d\omega/\omega^m) T_i(\omega, Q^2)$ occurs to be symmetric under $\omega \rightarrow -\omega$, because of the symmetry properties of T_i and the restriction for m Eq. (B.3). Thus,

$$\frac{d\omega}{\omega^m} T_i(\omega, Q^2) \xrightarrow{\omega \rightarrow -\omega} + \frac{d\omega}{\omega^m} T_i(\omega, Q^2), \quad i = 2, 3, L, \quad (\text{B.5})$$

and, in addition, we have used taken the discontinuity across the branch cut

$$\text{Im} T_i(\omega, Q^2) = \frac{1}{2i} (T_i(\omega + i\epsilon, Q^2) - T_i(\omega - i\epsilon, Q^2)), \quad i = 2, 3, L. \quad (\text{B.6})$$

Changing variables $\omega \rightarrow 1/x$ in Eq. (B.4) and using Eq. (B.3) for the r.h.s. of Eqs. (B.1), (B.2) one gets

$$\frac{1}{\pi} \int_0^1 dx x^{n-1} \text{Im} T_i(x, Q^2) = \sum_j C_{i,j} \left(n, \frac{Q^2}{\mu^2}, \alpha_s \right) A_{\text{nucl}}^j(n, \mu^2), \quad i = 2, 3, L. \quad (\text{B.7})$$

Applying the Lorentz projectors (2.27)–(2.29) to the optical theorem Eq. (2.9) and using Eq. (2.3) for hadronic tensor we obtain

$$\frac{1}{\pi} \text{Im} T_i(x, Q^2) = \frac{1}{x} F_i(x, Q^2), \quad i = L, 2, \quad (\text{B.8})$$

$$\frac{1}{\pi} \text{Im} T_3(x, Q^2) = F_3(x, Q^2). \quad (\text{B.9})$$

The combination of Eq. (B.7) with Eq. (B.8) concludes the derivation of Eqs. (2.30), (2.31) with special emphasis on the transformation properties of $T_{i\nu}$ under $\omega \rightarrow -\omega$ ($q \rightarrow -q$).

References

- [1] S. Moch, J.A.M. Vermaseren and A. Vogt, Nucl. Phys. B688 (2004) 101, hep-ph/0403192.
- [2] A. Vogt, S. Moch and J.A.M. Vermaseren, Nucl. Phys. B691 (2004) 129, hep-ph/0404111.
- [3] W.L. van Neerven and E.B. Zijlstra, Phys. Lett. B272 (1991) 127.
- [4] E.B. Zijlstra and W.L. van Neerven, Phys. Lett. B273 (1991) 476.
- [5] E.B. Zijlstra and W.L. van Neerven, Phys. Lett. B297 (1992) 377.
- [6] E.B. Zijlstra and W.L. van Neerven, Nucl. Phys. B383 (1992) 525.
- [7] S. Moch and J.A.M. Vermaseren, Nucl. Phys. B573 (2000) 853, hep-ph/9912355.
- [8] S. Moch, J.A.M. Vermaseren and A. Vogt, Phys. Lett. B606 (2005) 123, hep-ph/0411112.
- [9] J.A.M. Vermaseren, A. Vogt and S. Moch, Nucl. Phys. B724 (2005) 3, hep-ph/0504242.
- [10] ZEUS, S. Chekanov et al., Eur. Phys. J. C32 (2003) 1, hep-ex/0307043.
- [11] H1, C. Adloff et al., Eur. Phys. J. C30 (2003) 1, hep-ex/0304003.
- [12] H1, A. Aktas et al., Phys. Lett. B634 (2006) 173, hep-ex/0512060.
- [13] M.L. Mangano et al., (2001), hep-ph/0105155.
- [14] S.A. Larin, T. van Ritbergen and J.A.M. Vermaseren, Nucl. Phys. B427 (1994) 41.
- [15] S.A. Larin et al., Nucl. Phys. B492 (1997) 338, hep-ph/9605317.
- [16] A. Retey and J.A.M. Vermaseren, Nucl. Phys. B604 (2001) 281, hep-ph/0007294.
- [17] S. Moch, J.A.M. Vermaseren and A. Vogt, Nucl. Phys. B621 (2002) 413, hep-ph/0110331.
- [18] J. Blumlein and J.A.M. Vermaseren, Phys. Lett. B606 (2005) 130, hep-ph/0411111.
- [19] S. Moch, J.A.M. Vermaseren and A. Vogt, to appear.
- [20] A. Vogt, S. Moch and J. Vermaseren, Nucl. Phys. Proc. Suppl. 160 (2006) 44, hep-ph/0608307.
- [21] S. Moch, M. Rogal and A. Vogt, to appear.
- [22] Particle Data Group, W.M. Yao et al., J. Phys. G33 (2006) 1.
- [23] T. Muta, World Sci. Lect. Notes Phys. 57 (1998) 1.
- [24] G. 't Hooft and M. Veltman, Nucl. Phys. B44 (1972) 189.
- [25] C.G. Bollini and J.J. Giambiagi, Nuovo Cim. 12B (1972) 20.
- [26] J.F. Ashmore, Lett. Nuovo Cim. 4 (1972) 289.
- [27] G.M. Cicuta and E. Montaldi, Nuovo Cim. Lett. 4 (1972) 329.
- [28] G. 't Hooft, Nucl. Phys. B61 (1973) 455.
- [29] W.A. Bardeen et al., Phys. Rev. D18 (1978) 3998.
- [30] S.A. Larin and J.A.M. Vermaseren, Phys. Lett. B259 (1991) 345.
- [31] S.A. Larin, Phys. Lett. B303 (1993) 113, hep-ph/9302240.
- [32] S.G. Gorishnii, S.A. Larin and F.V. Tkachev, Phys. Lett. 124B (1983) 217.
- [33] S.A. Larin, F.V. Tkachev and J.A.M. Vermaseren, NIKHEF-H-91-18.
- [34] P. Nogueira, J. Comput. Phys. 105 (1993) 279.
- [35] J.A.M. Vermaseren, Nucl. Phys. Proc. Suppl. 116 (2003) 343, hep-ph/0211297.

- [36] J.A.M. Vermaseren and M. Tentyukov, Nucl. Phys. Proc. Suppl. 160 (2006) 38.
- [37] T. van Ritbergen, A.N. Schellekens and J.A.M. Vermaseren, Int. J. Mod. Phys. A14 (1999) 41, hep-ph/9802376.
- [38] Y.L. Dokshitzer, G. Marchesini and B.R. Webber, Nucl. Phys. B469 (1996) 93, hep-ph/9512336.
- [39] W.L. van Neerven and A. Vogt, Nucl. Phys. B603 (2001) 42, hep-ph/0103123.
- [40] A.L. Kataev, G. Parente and A.V. Sidorov, Nucl. Phys. B573 (2000) 405, hep-ph/9905310.
- [41] A.L. Kataev, G. Parente and A.V. Sidorov, Phys. Part. Nucl. 34 (2003) 20, hep-ph/0106221.
- [42] W.G. Seligman et al., Phys. Rev. Lett. 79 (1997) 1213.
- [43] J.A.M. Vermaseren, Comput. Phys. Commun. 83 (1994) 45.
- [44] D. Binosi and L. Theussl, Comput. Phys. Commun. 161 (2004) 76, hep-ph/0309015.